BURCU BALCI

ATILIM UNIVERSITY 2021

SYNTHESIS OF CHEMILUMINESCENT COMPOUNDS AND THEIR USAGE IN METAL ION RECOGNITION AND BLOOD DETECTION

THE GRADUATE SCHOOL OF NATURAL AND APPLIED SCIENCES
OF
ATILIM UNIVERSITY

BURCU BALCI

A MASTER OF SCIENCE THESIS
IN
THE DEPARTMENT OF CHEMICAL ENGINEERING

JULY 2021

SYNTHESIS OF CHEMILUMINESCENT COMPOUNDS AND THEIR USAGE IN METAL ION RECOGNITION AND BLOOD DETECTION

A THESIS SUBMITTED TO
THE GRADUATE SCHOOL OF NATURAL AND APPLIED SCIENCES
OF
ATILIM UNIVERSITY

BY

BURCU BALCI

IN PARTIAL FULFILLMENT OF THE REQUIREMENTS
FOR
THE DEGREE OF MASTER OF SCIENCE
IN
THE DEPARTMENT OF CHEMICAL ENGINEERING

JULY 2021

Approval of the Graduate School of Natural and Applied Sciences, Atılım University.

_____

Prof. Dr. Ender Keskinkılıç
Director

I certify that this thesis satisfies all the requirements as a thesis for the degree of the **Master of Sciences in Chemical Engineering and Applied Chemistry at Atılım University**.

_____

Prof. Dr. Şeniz Özalp Yaman
Head of Department

This is to certify that we have read this thesis "SYNTHESIS OF CHEMILUMINESCENT COMPOUNDS AND THEIR USAGE IN METAL ION RECOGNITION AND BLOOD DETECTION" submitted by BURCU BALCI and that in our opinion it is fully adequate, in scope and quality as a thesis for the degree of Master of Science.

_____

Prof. Dr. Atilla Cihaner
Supervisor

Examining Committee Members:

Prof. Dr. Murat Kaya
Department of Chemical Engineering,
Atılım University _____

Prof. Dr. Atilla Cihaner
Department of Chemical Engineering,
Atılım University _____

Assoc. Prof. Dr. Merve İçli Özkut
Department of Chemistry,
Ankara University _____

Date: 09.07.2021

I hereby declare that all information in this document has been obtained and presented in accordance with academic rules and ethical conduct. I also declare that, as required by these rules and conduct, I have fully cited and referenced all materials and rules that are not original to this work.

Name, Last Name : Burcu Balcı

Signature :

ABSTRACT

SYNTHESIS OF CHEMILUMINESCENT COMPOUNDS AND THEIR USAGE IN METAL ION RECOGNITION AND BLOOD DETECTION

Balcı, Burcu
MSc., Department of Chemical Engineering
Supervisor: Prof. Dr. Atilla Cihaner

July 2021, 66 pages

Luminescent compounds have gained great importance recently due to their wide application areas. In addition, chemiluminescent compounds have been used for many studies in analytical chemistry due to their high luminescence sensitivity. In this thesis, a new series of chemiluminescent compounds, namely 5,8-di(furan-2-yl)-2,3-dihydrophthalazine-1,4-dione (F_2B-Lum), 5,8-di(selenophene-2-yl)-2,3-dihydrophthalazine-1,4-dione (S_2B-Lum) and 5,7-di(selenophen-2-yl)-2,3-dihydrothieno[3,4-d] pyridazine-1,4-dione (S_2T-Lum), was synthesized via electron donor-acceptor-donor approach. Their structures were confirmed by using NMR, FTIR and HRMS techniques. Then, the chemiluminescence reactions of compounds with hydrogen peroxide in an alkaline solution (0.1 M NaOH(aq)) in the presence of different metal ions, hemin and blood samples were investigated and the results were compared with luminol. As expected, the compounds were sensitive to copper(II), iron(III) ions and blood. It can be easily concluded that the corresponding compounds as new derivatives of luminol are potential candidates for the detection of blood findings in forensic science. In addition, the sensitivity of the compounds to copper(II) ion makes them usable for copper ion recognition in analytical applications. Furthermore, cyclic voltammetry technique was used to investigate the redox behaviors of the compounds and they exhibited irreversible oxidation peaks.

Also, reactive oxygen species can be detected by using these compounds via square wave potential method by applying an external potential of -1.05 V. Finally, among the compounds, S_2T-Lum was successfully polymerized electrochemically. The corresponding polymer PS_2T-Lum can be a precious member of luminol type polymers since it is electroactive and bears chemiluminescent active appendages in its polymeric structure.

Keywords: Blood detection, chemiluminescence, ion recognition.

ÖZ

KEMİLÜMİNESANS BİLEŞİKLERİN SENTEZİ VE METAL İYONU TANIMA VE KAN TESPİTİNDE KULLANIMLARI

Balcı, Burcu
Yüksek Lisans, Kimya Mühendisliği Bölümü
Tez Yöneticisi: Prof. Dr. Atilla Cihaner

Temmuz 2021, 66 sayfa

Lüminesan bileşikler, geniş uygulama alanları sebebiyle son zamanlarda büyük önem kazanmıştır. Ayrıca, kemilüminesan bileşikler, yüksek lüminesans hassasiyetlerinden dolayı analitik kimyada birçok çalışmada kullanılmıştır. Bu tezde elektron verici-alıcı-verici yaklaşımı ile, isimleri 5,8-di(furan-2-il)-2,3-dihidroftalazin-1,4-dion (F_2B-Lum), 5,8-di(selenofen-2-il)-2,3- dihidroftalazin-1,4-dion (S_2B-Lum) ve 5,7-di(selenofen-2-il)-2,3-dihidrotiyeno[3,4-d] piridazin-1,4-dion (S_2T-Lum) olan, yeni bir kemilüminesan bileşik serisi sentezlenmiştir. Yapıları NMR, FTIR ve HRMS teknikleri kullanılarak doğrulanmıştır. Daha sonra, alkali çözeltide (0,1 M NaOH(sulu)) bileşiklerin hidrojen peroksit ile farklı metal iyonları, hemin ve kan örnekleri varlığında kemilüminesans tepkimeleri araştırılmış ve sonuçlar luminol ile karşılaştırılmıştır. Beklendiği gibi, bileşiklerin bakır(II), demir(III) iyonlarına ve kana duyarlı olduğu gözlenmiştir. Yeni luminol türevleri olarak ilgili bileşiklerin, adli bilimde kan bulgularının tespiti için potansiyel adaylar olduğu sonucuna kolaylıkla varılabilir. Ek olarak, bileşiklerin bakır(II) iyonuna duyarlılığı, onları analitik uygulamalarda bakır iyonu tanıma için kullanılabilir hale getirmiştir. Ayrıca, bileşiklerin redoks davranışlarını araştırmak için döngülü voltametri tekniği kullanılmış ve tersinmez yükseltgenme sinyalleri göstermişlerdir.

Ayrıca bu bileşikler kullanılarak -1.05 V'luk bir dış potansiyel uygulanarak kare dalga potansiyel yöntemi ile reaktif oksijen türleri tespit edilebilmektedir.Son olarak bileşiklerden S_2T-Lum elektrokimyasal olarak başarılı bir şekilde polimerleştirilmiştir. İlgili polimer PS_2T-Lum, elektroaktif olduğu ve polimerik yapısında kemilüminesan aktif uzantılar taşıdığı için luminol tipi polimerlerin değerli bir üyesi olabilir.

Anahtar Kelimeler: Kan bulgusu, kemilüminesans, iyon tanıma.

To my family

ACKNOWLEDGMENTS

These extraordinary people in my life are the biggest factor in my coming to this stage. Thanks to them, I have overcome many difficulties. Firstly, I give special thanks to my supervisor Prof. Dr. Atilla Cihaner for his patience, interest, guidance and for not sparing his support throughout of this study. I am very lucky to know him.

I would like to thank for my examining committee members, Prof. Dr. Murat Kaya and Assoc. Prof. Dr. Merve İçli Özkut for their participation, interests, and suggestions.

I would also like to my endless thanks to Asst. Prof. Dr. Salih Ertan for his help and interest in the laboratory, and to my friends Bengisu Varlık, Büşra Kesimal, Hasan Berk and Mert Topcuoğlu for their helps and valuable time shared with me.

I would like to thank members of the Atılım Optoelectronic Materials and Solar Energy Laboratory (ATOMSEL) research group and the Chemical Engineering Department of Atılım University. Thank you very much to Prof. Dr. Ahmet M. Önal for his support and especially Deniz Çakal for helps, support, interest, and her precious time for me at Chemistry Department of Middle East Technical University (METU).

I would like to thank my parents Sultan and Cengiz Balcı, my brother Barış Can Balcı and my grandparents Mesudiye and Necati Sinan for their love, motivation and supports in my decisions. During this process, they did not leave me alone and shared both my happiness and sadness with me.

Finally, I would like to thank the Scientific and Technological Research Council of Turkey (TUBITAK, Grand number: 118Z067) for its financial support.

TABLE OF CONTENTS

LIST OF TABLES

LIST OF FIGURES

LIST OF SYMBOLS/ABBREVIATIONS

A	Absorption Value
ACN	Acetonitrile
a.u	Absorbance Unit
A.U.	Arbitrary Unit
$BF_3.Et_2O$	Borontrifluoro diethylether
$CDCl_3$	Deuterated Chloroform
CE	Counter Electrode
CL	Chemiluminescence
D-A-D	Donor-Acceptor-Donor
DCM	Dicloromethane
DMSO	Dimethyl sulfoxide
DNA	Deoxyribo Nucleic Acid
ECL	Electrochemiluminescence
F	Area of Emission Spectrum
FTIR	Fourier Transform Infrared
F_2B-Lum	5,8-di(furan-2-yl)-2,3-dihydrophthalazine-1,4-dione
F_2-EHPI	2-(2-ethylhexyl)-4,7-di(furan-2-yl)isoindoline-1,3-dione
F_2-PA	4,7-di(furan-2-yl)isobenzofuran-1,3-dione
HRMS	High Resolution Mass Spectrometry
IR	Infrared
ITO	Indium Tin Oxide
n	Refractive Index of the Solvent
NMR	Nuclear Magnetic Resonance
PMT	Photomultiplier Tube
QY	Quantum Yield
RE	Reference Electrode
S_2B-Lum	5,8-di(selenophene-2-yl)-2,3-dihydrophthalazine-1,4-dione

S_2-EHPI	2-(2-ethylhexyl)-4,7-di(selenophen-2-yl)isoindoline-1,3-dione
S_2-EHTP	5-(2-ethylhexyl)-1,3-di(selenophen-2-yl)-4H-thieno[3,4-c]pyrrole-4,6(5H)-dione
S_2T-Lum	5,7-di(selenophen-2-yl)-2,3-dihydrothieno[3,4-d]pyridazine-1,4-dione
S_2-PA	4,7-di(selenophen-2-yl)isobenzofuran-1,3-dione
S_x	Singlet States
TBAH	Tetrabutylammonium hexafluorophosphate
THF	Tetrahydrofuran
TLC	Thin Layer Chromatography
T_x	Triplet States
UV	Ultraviolet
Vis	Visible
WE	Working Electrode
Φ_{CL}	Chemiluminescence Quantum Yield

CHAPTER 1

INTRODUCTION

1.1 Luminescence

Luminescence is the emission of electromagnetic radiation. It can take place in the UV (100 nm-380 nm), visible (380 nm - 760 nm) and IR (760 nm-1000 nm) regions [1]. A version of the diagram, which was firstly proposed in 1933 by the Polish physicist Aleksander Jablonski to describe the luminescence phenomena of many organic compounds [2], given in Figure 1.1 called the Jablonski diagram. The diagram bearing different electronic energy levels represents the intermolecular energy transfer. According to the diagram, luminescence occurs when the reaction product returns from electronically excited state (high energy) to the basic state (low energy). If the excited reaction product returns from the lowest singlet excited state (S_1) to its ground state (S_0), the radiation occurs, which is called fluorescence or chemiluminescence. If the electron returns from the triplet excited state (T_1) to the ground state (S_0), this is called phosphorescence [3].

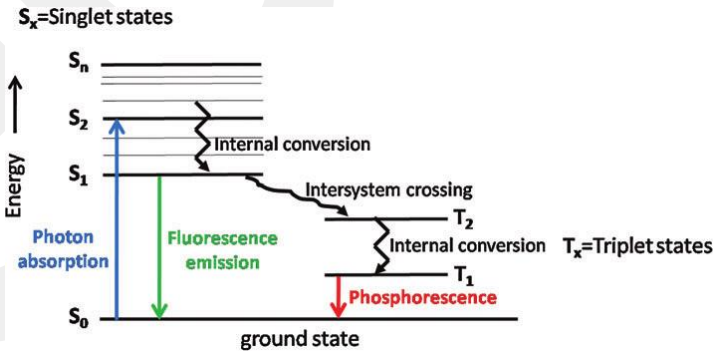

Figure 1.1 Jablonski Energy Diagram [4]

There are some types of luminescence such as absorption (photoluminescence), heating (thermoluminescence), electric current (electroluminescence), living organism (bioluminescence), chemical reaction (chemiluminescence), etc. These luminescence types get the names from source of their emission.

1.1.1 Chemiluminescence (CL)

In chemiluminescence (CL) process, the luminescence is initiated by an irreversible chemical reaction. If, one of the excited reaction products returns to its ground state (S_0), radiation occurs. This radiation can be in different intensities, half-life times and wavelengths. CL reaction can emit light in the UV and IR range as well as in the visible region [3].

There are several ways for a molecule can return from an excited state to a ground state (Figure 1.1). For observing emission from a chemical reaction, three essential energetic requirements need to be complete. The first, the reaction path chosen for passing to the excited state must be energetically favorable. An important part of the total number of molecules participating in the reaction should reach the excited state. Another requirement is that the related reaction is exothermic. Finally, there must be a suitable deactivation route for CL emission. While radiative CL emission is dominate, non-radiative processes such as intramolecular or intermolecular energy transfer, molecular dissociation, isomerization or physical quenching should be minimal [5].

The intensity of the CL emission depends on the reaction rate and the process efficiency. The CL quantum yield (Φ_{CL}) can be defined as (1.1) [5]:

$$\Phi_{CL} = \frac{\text{total number of photons emitted}}{\text{number of molecules reacting}} \qquad (1.1)$$

A CL reaction can be generated by two type mechanisms known in the literature (Figure 1.2). These are direct and indirect CL reactions. In a direct reaction a CL precursor (A) and an oxidant (B) in the presence of some cofactors usually react to form a product or intermediate (P*).

This product is in a primary excited state and performs the CL reaction with emission of a photon when it returns to ground state. Except for the direct reaction, in an indirect reaction, the excited product does not emit light, but it transfers its energy to another receiver (F*) and this receiver performs the CL reaction. The CL precursor is a substrate that converted into the electronically excited molecule, which is responsible for light emission in the direct reaction or is the energy transfer donor in the indirect reaction. Catalyst such as metal ions, reduces the activation energy and provides a suitable medium for increasing the efficiency of CL reaction. Cofactors are used sometimes to convert one or more substrates into a form capable of reacting with the catalyst [6].

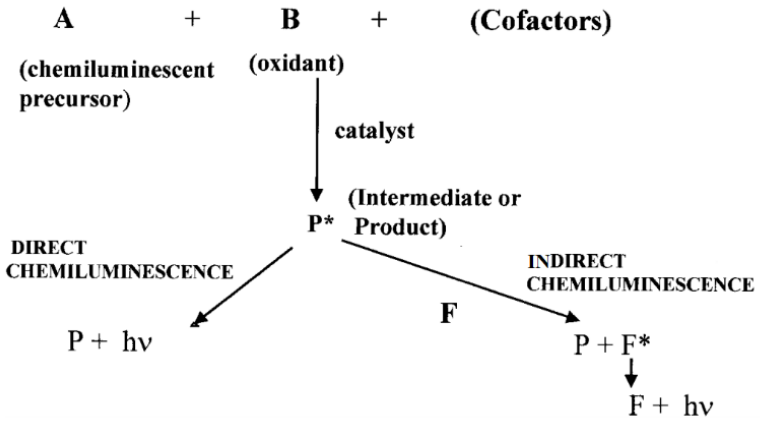

Figure 1.2 Types of CL reactions [6]

1.1.1.1 Historical Development of CL Compounds

Glows in the sea, shining of wood, dead fish, and body were first observations about luminescence at 1600s. These first examples of luminescence are based on living organisms and named as bioluminescence. Some living organisms such as glowworm, octopus, sea violets and jellyfish are examples of bioluminescence (Figure 1.3). Luciferin, which is found in glowworm and bacteria, reacts with oxygen under the catalysis of lucipherase enzyme and reaches excited state. Therefore, this luminescence occurs as a kind of CL [7]. Some bioluminescence examples are given in Figure 1.3.

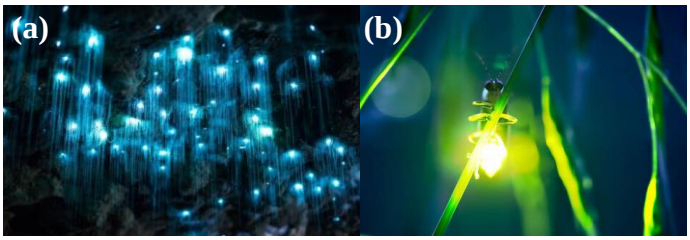

Figure 1.3 (a) Bioluminescece [8], (b) a firefly that emits bioluminescent glow [9]

Lophine (2,4,5-triphenylimidazole) known in the literature is the first non-living, synthetic substance to show CL properties. It was studied by Radziszewski in 1877 [10]. The CL mechanism of lophine (Figure 1.4) and some other compounds that have CL properties (Figure 1.5) are given in below.

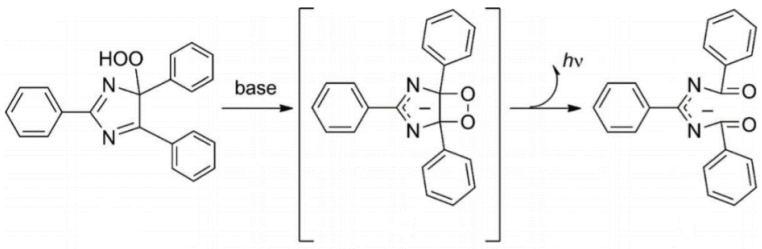

Figure 1.4 CL mechanism of lophine [11]

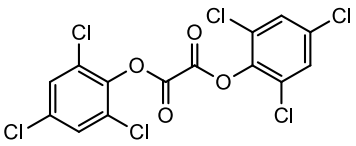

bis(2,4,6-trichlorophenyl) oxalate

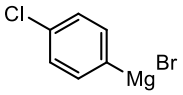

p-Chloro Phenyl magnesium bromide

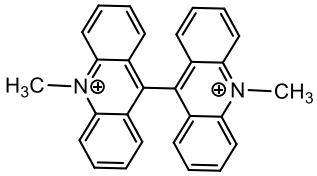

Dimethylbisacridium nitrate

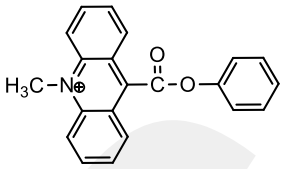

Acridinium ester

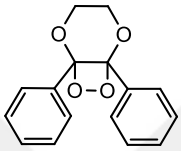

2-Phenyl-3--(4'-hidroxyphenyl)-1-4-dioxane

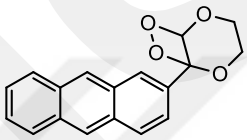

1-(anthracen-2-yl)-2,5,7,8-tetraoxabicyclo[4.2.0]octane

Figure 1.5 Some CL compounds

CL compounds have received much attention in the field of analytical and material sciences due to their high sensitivity, high luminescence efficiency, and simple instrumentation.

1.2 Luminol (3-aminophthalhydrazide)

3-aminophthalhydrazide (luminol) is a chemical compound which has a CL property. It is a cyclic acyl-hydrazide and has a yellow crystalline structure [5]. It was found in 1908 by German Scientist Schimitz [12].

Luminol is one of the mostly used CL materials. CL property of luminol was proved in 1928 by Albrecht. [13]. Luminol becomes ready to react in basic medium and named of its structure as diazaquinone dianion. Luminol is poorly soluble in dilute acids and emits very strong blue light. CL is not observed when oxidizing agents are added. However, luminol is readily soluble in alkaline and the solution does not emit. However, when oxidized, it glows an intense blue [13]. When it interacts with an oxidizing substance such as hydrogen peroxide, it reaches excited state (S_1).

During this reaction N_2 gas releases to the environment. Eventually, in the presence of a suitable catalyst, it gives its energy in the form of light when the substance returns from excited state (S_1) to ground state (S_0). Therefore, a blue light is observed [5]. The blue-green light obtained from the CL reaction of luminol is observed between 375 nm and 500 nm [14]. CL mechanism and the reaction stages of luminol are shown in Figure 1.6.

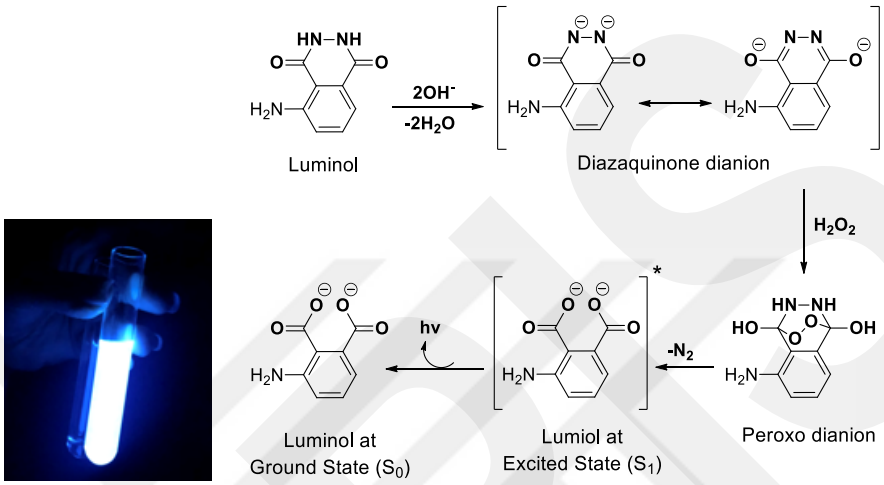

Figure 1.6 CL emission and mechanism of luminol

In order to luminol pass into the peroxo dianion form, there must be an oxidizer such as H_2O_2 in the environment (Figure 1.6). The $O_2^{-\bullet}$ radicals formed in the solution of H_2O_2 form a tense bridge in the structure. The presence of Fe^{3+} ions in the environment speeds up the formation of $O_2^{-\bullet}$ radicals. The steps of the mechanism of conversion of H_2O_2 to $O_2^{-\bullet}$ radicals are given in equations 1.2-1.5 [15].

$$H_2O_2 \rightarrow HO^{\bullet} + HO^{\bullet} \quad (1.2)$$

$$H_2O_2 + HO^{\bullet} \rightarrow H_2O + HOO^{-\bullet} \quad (1.3)$$

$$HO^{\bullet} + HOO^{-\bullet} \rightarrow H_2O + O_2^{-\bullet} \quad (1.4)$$

$$Fe^{3+} + H_2O_2 \rightarrow Fe^{2+} + HOO^{-\bullet} + H^{+} \quad (1.5)$$

While in the absence of a catalyst, the light is too faint to be seen with the naked eye and continues for a long time. In the presence of a catalyst, a faster and more visible light occurs.

However, although it is suggested that the effect of the catalyst in the mechanism is as in equation 1.5, its actual role is not fully known. The CL reaction of luminol can be catalyzed by various metal complexes [16]. Also, the light emission depends on several factors such as pH, temperature, types of oxidants and metal ion catalysts [17].

1.2.1 Electrochemiluminescence (ECL) of Luminol

Electroluminescence is an emitted light by resulting from electrical current. When electrons hit a solid or liquid, the light is emitted. Electroluminescence, which is a glow in various colors, arises from a flow of current through partially empty tubes of gas. This luminescence type is commonplace today. For example, it is used commonly in neon lights at advertising signs [7].

If luminescence is produced by electrode reactions, it is also called "electrochemiluminescence" (ECL). ECL was researched firstly by Hercules in 1964 [18]. ECL is a light emission at electrodes in electrochemical cells due to redox reactions of electrogenerated species in solution. The reaction system for an ECL can be explainable as including a solution containing reactants A and D, a supporting electrolyte, for example, tetrabutylammonium perchlorate in acetonitrile and working electrode [19]. The reaction stages are given below.

$$A + e^- \rightarrow A^{-\bullet} \quad \text{(reduction at the electrode)} \quad (1.6)$$

$$D - e^- \rightarrow D^{+\bullet} \quad \text{(oxidation at the electrode)} \quad (1.7)$$

$$A^{-\bullet} + D^{+\bullet} \rightarrow {}^1A^* + D \quad \text{(excited state formation)} \quad (1.8)$$

$$ {}^1A^* \rightarrow A + h\nu \quad \text{(light emission)} \quad (1.9)$$

ECL compounds have become an important material in analytical chemistry for detection of low concentrations of analyte samples. Additionally, these compounds are commonly used in clinical and biomedical diagnostics [20], [21], [22].

In alkaline solution, the luminol undergoes electro-oxidation with a single electron. This oxidation causes to form a diazaquinone compound. In the presence of hydrogen peroxide, an excited compound called as 3-aminophthalate reacts with peroxide and emits light at 425 nm. Therefore, luminol and its derivatives can be used for the determination of hydrogen- and other peroxides.

This property enables luminol to be used as a H_2O_2 sensor [23]. This ECL reaction mechanism is shown in detail in Figure 1.7.

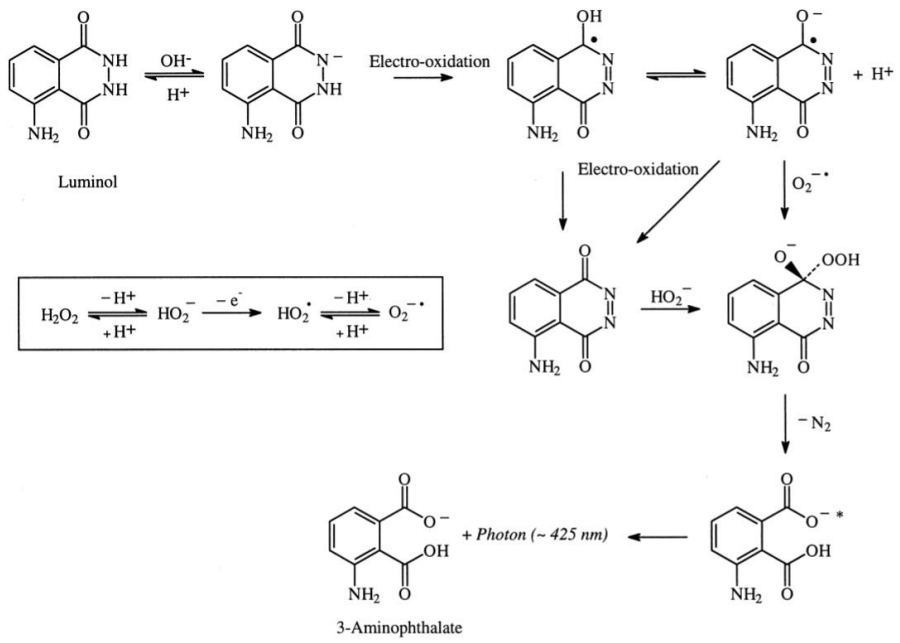

Figure 1.7 ECL mechanism of luminol [23]

1.2.2 Application Areas of Luminol

Today, interest in the use of CL systems due to their high luminescence sensitivity and low cost is considerable in analytical chemistry. Luminol is the most widely used compound among the CL compounds. Luminol is used in determination of biologically active, easily oxidized and indirectly determined substances (heme compounds, peroxidases, oxidants as H_2O_2, inhibitors as Ag(I), ascorbic, acid, carboxylic acids, amines, etc.), substances converted into H_2O_2 (glucose, etc.), some metal ions and complexes (Co(II), Cu(II), Fe(III) etc.) [6]. It is also used in immunoassay determination and DNA probe trials [24], food [25], pesticide [26], and air pollution analysis [27].

Luminol is an effective compound used in the determination of biologically active substances. The reaction pathway of the detection mechanism of glucose as one of these substances is given in (1.10) and (1.11) [28]. Glucose is oxidized to gluconic acid with the catalytic effect of glucose oxidase enzyme (GOD). In the meantime, the substrate oxygen is transformed to H_2O_2. Hematin acting as a catalyst converts H_2O_2 back to O_2. Luminol is oxidized by O_2 in the presence of hematin, producing a CL emission [29].

$$\text{Glucose} + O_2 \rightarrow \text{Gluconic Acid} + H_2O_2 \tag{1.10}$$

$$\text{Luminol} + H_2O_2 \rightarrow \text{3-Aminophthalic Acid} + h\nu \tag{1.11}$$

Many metal ions such as iron, cobalt, chromium, nickel, copper and manganese catalyze the CL reaction of luminol. Thus, by measuring the resulting radiation, the number of substances used as catalysts can be determined [30], [31], [32], [33], [34]. Luminol plays a major role in the development of highly sensitive biosensors because it can be used in analytic determination by its ECL property. [35]. For this purpose, it can be used in the sensor of some biologically active substances such as glucose, protein and for cancer biomarker detection. Gold nanoparticles [35], chitosan coated Fe_3O_4 [36], Pd and Pt [37], ZnO [38], MnO_2 [39] nanoparticles and TiO_2/Carbon nanotubes nanocomposites [40] were used as catalysts in the CL reaction. The ECL signal of luminol can be highly increased with the use of the catalyst, resulting in increased sensitivity. As an example, as seen in Figure 1.8, gold nanoparticles are prepared by a sol-gel method and placed on the electrode. Glucose oxidase (GOx) is adsorbed on the surface of gold nanoparticles. It reacts with glucose to form H_2O_2 and glucose is oxidized. Then, the formed H_2O_2 reacts with luminol to generate the ECL signal and the resulting luminescence is measured. Therefore, this system has proven to be efficient for glucose detection.

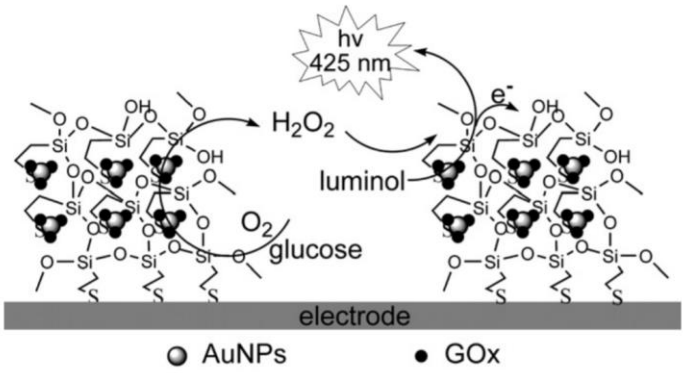

Figure 1.8 Principle of glucose biosensor based on gold nanoparticles (AuNP)-catalyzed luminol ECL [35]

1.2.3 Luminol in Forensic Science

Luminol is the most widely used and known compound in forensic science thanks to its especially CL feature. It has attracted great attention in this science due to its photo- and thermal- stability, chemical behavior in protic polar media. The first studies of luminol on blood findings were made in 1937 [41]. Then, it continued to be used effectively in detection of blood for more than forty years [5].

Most confirmatory analysis of blood identification is based on the detection of hemoglobin. Hemoglobin is the substance that gives red color to blood. Additionally, it is the oxygen carrier protein and is located in the erythrocytes. Each hemoglobin contains a heme molecule (also called ferroprotoporphyrin). The heme molecule consists of a protoporphyrin IX and an iron atom [42]. Iron in the organism is in the form of Fe^{2+}. Because hemoglobin is protected against denaturation within red blood cells. This state of hemoglobin containing Fe^{2+} atoms is called heme. When the iron leaves the organism and accumulates on a substrate, the blood undergoes a series of degradation processes and, after oxidation, it becomes Fe^{3+}. In this case, the color of the blood turns brown, and hemoglobin is called hematin (Figure 1.9).

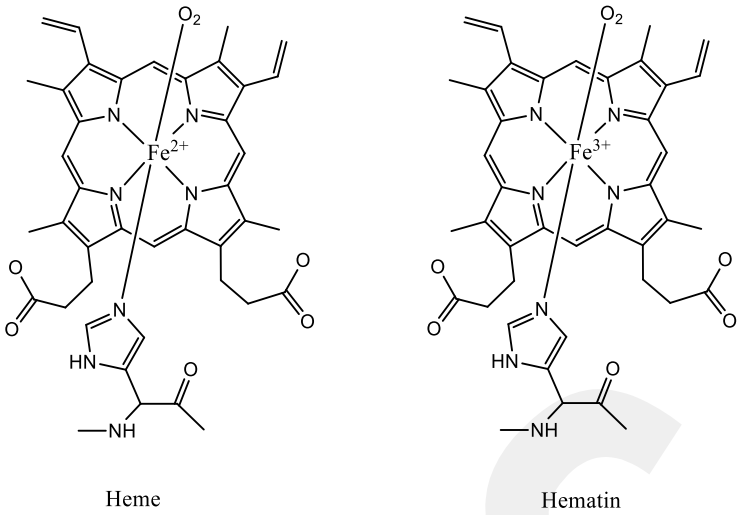

Figure 1.9 Hemoglobin structure inside the organism (HEME) and outside the organism (HEMATIN)

Fe^{3+} ions in hematin groups catalyze both the degradation reaction of peroxide and the oxidation reaction of luminol. Because of hematin groups found in blood findings, when the luminol solution is applied on a blood sample, CL reaction takes place. The blue light resulting from the reaction can be easily seen in the dark (Figure 1.10).

Thus, luminol can be used to detect blood even if it is too small to be seen in a dark environment. However, luminol has some disadvantages. Although there is no blood in the environment, luminol reaction can be catalyzed by some metals other than Fe^{3+} ion. In addition, CL reaction of luminol has a high-energy blue light, which causes several damaging effects on the DNA and causes DNA loss in the blood findings [5].

Figure 1.10. (a) Blood stains on the crime scene are not visible by the naked eye in daylight. (b) Visible blue light is obtained from blood samples after applying luminol in a dark environment at the crime scene.

The blue glow observed when luminol solution is applied does not always prove the presence of blood. There are several other substances besides the blood that can catalyze the oxidation of luminol. It can be oxidized by the chemicals in bleach, such as sodium chlorate; urine can also trigger the reaction due to the presence of trace amount of blood. Additionally, peroxidase enzymes found in faeces and horseradish can set off the CL [43].

1.2.4 Polyluminol

Conducting polymers have common usage area because of their electronic and optical properties: sensors, electrochromic devices [44], light emitting diodes, transistors [45, 46], photovoltaic cells [47], etc. Many aniline derivatives have been studied to obtain functional polyaniline derivatives [48]. Luminol is an aniline derivative. However, it has not yet been possible to develop luminol and pyridazine based polymers as an electroactive film because of solubility problems, limited thickness of the polymer film and the complex polymerization mechanism of luminol constrains their use.

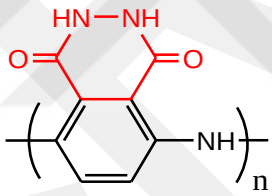

Figure 1.11 Structure of polyluminol

1.3 Luminol Type Compounds

Considering the disadvantages of luminol such as very low quantum yield of around 1-5% [49], insolubility, disrupting the DNA structure [5], its misleading results in blood tests [43], designed new compounds to eliminate these negativities are very necessary. For this purpose, some compounds were synthesized successfully with structural changes on luminol. Analogs in which the amino group was replaced by other substituents were generally found to be CL. [50] These compounds are different according to their light-producing ability. For example, when compared with luminol, compounds (1) and (2) [51] have low efficiency. However, compounds (3) [52] and (4) [53] are more CL than luminol.

It has been shown that energy transfer occurs in the CL of hydrazides (5), which are bound to some highly fluorescent groups. [54]. A new luminol type CL probe (6) was developed that can be used to detect reactive oxygen species besides blood [55]. Asil et al. were synthesized highly sensitive compound (8) towards Fe^{3+} ions. This sensitivity makes them good candidates for forensic applications to detect blood spots [56], compound (10) was designed a low energy emitting material via the CL energy transfer, which covers almost the entire visible region (400 nm-700 nm) [57], (11) [58], (12) [59], (13) [60], (14) [61].

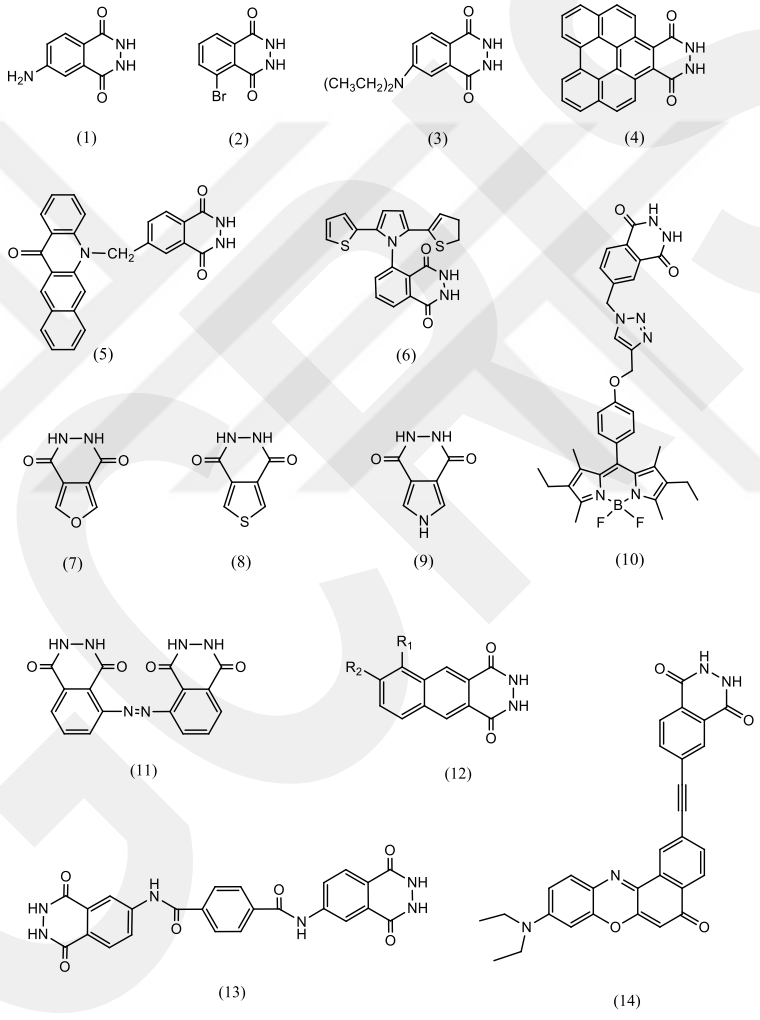

Figure 1.12 Some luminol derivatives

The effect of substituents on the CL intensities is important, and it is based on the electrometric effects of the substituents. For example, the position of the substituent of isoluminol (Figure 1.13), affects the CL intensity negatively. When the CL intensity of luminol is 100, that of isoluminol is 4. In addition, some derivatives with different substituents (5-NO, 5-H, 5-OH, 5-NH) have also been reported to have lower CL properties compared to luminol [62].

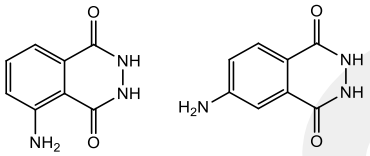

Figure 1.13. Structures of luminol and isoluminol

1.3.1 Electron Donor-Acceptor-Donor (D-A-D) Type Luminol Analogs

D-A-D type different alternative compounds to luminol are designed but these are very few in the literature. D-A-D type compounds, in other words, trimeric compounds, unlike luminol and its derivatives, can easily polymerize without degrading the CL unit. In this system, both light emission and polymerization can be controlled electrochemically. In addition, CL groups added to trimeric systems are thought to make the materials suitable for use as sensors. Redox driven CL compounds (15) [63] and (17) [64] based on thienyl and pyridazine systems, was soluble compounds both in organic media and basic aqueous solution. Additionally, these monomers can be polymerized successfully via electrochemical polymerization (Figure 1.14).

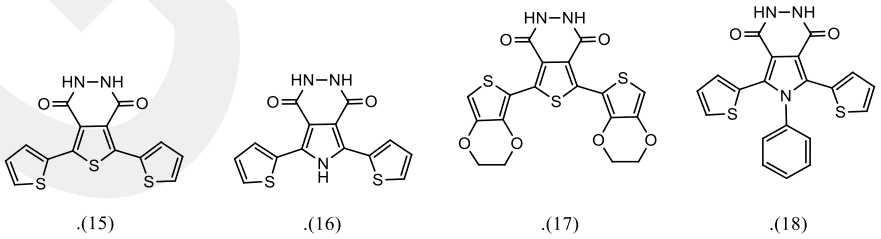

Figure 1.14. Some CL D-A-D type compounds

1.4 Aim of This Work

Luminescent compounds have recently been importance in many areas. Luminol is a chemiluminescent compound known in the literature and used frequently in various applications, especially in forensic science. However, luminol has some disadvantages. Thus, new compounds designed to eliminate these disadvantages are required. There are some modified structures in the literature. Unfortunately, the expect attention could not be obtained because they have multiple reaction steps Therefore, in this study, it was aimed to introduce new members of CL compounds, namely 5,8-di(furan-2-yl)-2,3-dihydrophthalazine-1,4-dione (F_2B-Lum), 2,3-dihydro-5,8-di(selenophen-2-yl)phthalazine-1,4-dione (S_2B-Lum) and 2,3-dihydro-5,7-di(selenophen-2-yl)selenopheno[3,4-d]pyridazine-1,4-dione (S_2T-Lum) (Figure 1.15), with shorter experimental steps to the literature. Compounds were designed in D-A-D form so that they can be easily polymerized. It is hoped that the obtained materials can be used in forensic for blood detection. In addition to blood tests, the sensitivity of the synthesized compounds to metal ions was tested and thus it was be understood whether they can be used as sensors.

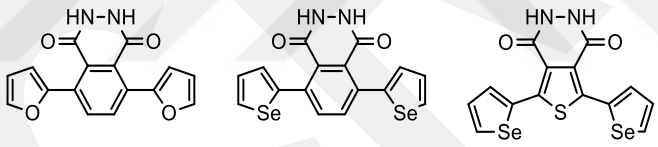

F_2B-Lum S_2B-Lum S_2T-Lum

Figure 1.15. Structures of F_2B-Lum, S_2B-Lum and S_2T-Lum

CHAPTER 2

EXPERIMENTAL

2.1 Materials

- 3,6-dibromophthalic anhydride (Tokyo Chemical Industry, >98.0%)
- 4,7-dibromo-2-(2-ethylhexyl) isoindoline-1,3-dione (Luminescence Technology Corp)
- 1,3-dibromo-5-(2-ethylhexyl)-4H-thieno[3,4-c]pyrrole-4,6(5H)-dione (Aldrich)
- 2-(Tributylstannyl)furan (Sigma-Aldrich, 97.0%)
- 2-(Tributylstannyl)selenophene (METU)
- 1-4 Dioxane (Merck, ≥99.0%)
- Acetonitrile (ACN) (Sigma-Aldrich, ≥99.9%)
- Ag/AgCl electrode
- Aluminum plates for TLC (Merck, 20x20, Silica gel 60 F_{254})
- Benzophenone (Sigma-Aldrich, 99.0%)
- Boron trifluoride (BF_3)
- Bis(triphenylphosphine) palladium (II) dichloride (Sigma-Aldrich, ≥98.0%)
- Chloroform-D1 (Merck, deuteration degree min. 99.8%)
- Dichloromethane (DCM) (ISOLAB, ≥99.9%)
- Dimethyl Sulfoxide (DMSO) (LAB-SCAN, 99.5%)
- Dimethyl Sulfoxide D6 (Eurisotop, deuteration degree min. 99.8%
- Dry magnesium sulfate ($MgSO_4$) (Sigma-Aldrich, ≥97.0%)
- Ethanol (ISOLAB, ≥99.9%)
- Ethyl Acetate (ISOLAB, ≥99.5%)
- Glacial acetic acid (Carlo Erba, 99.5%)
- Hemin (Fluka, >98.0%)

- Hexane (Sigma-Aldrich, ≥95.0%)
- Hydrazinium hydroxide (Merck, 80.0%)
- Hydrogen Peroxide (Merck, 35.0%)
- Indium tin oxide coated glass (ITO, Delta Tech. 8-12 Ω, 0.7 cm - 5 cm)
- Platinum disc electrode (electrode area: 0.02 cm^2)
- Platinum wire
- Potassium Dichromate (Sigma-Aldrich, 99.9%)
- Potassium Permanganate (Sigma-Aldrich, 99.9%)
- Silica gel (SiO_2) (Acros, 0.060-0.200 mm, 60 A)
- Sodium Hydroxide (Sigma-Aldrich, ≥98.0%)
- Sodium Metal (Merck, 99.0%)
- Sulfuric Acid (H_2SO_4(aq)) (Merck, 95-98%)
- Tetrabutylammonium hexafluorophosphate (TBAH) (Sigma-Aldrich, ≥99.0%)
- Tetrahydrofuran (THF) (Carlo Erba, ≥99.9%)
- Metal Cations Sources (Sigma-Aldrich); $AgNO_3$, $Al(NO_3)_3.9H_2O$, $Cd(ClO_4)2.xH_2O$, $Co(NO_3)_2.6H_2O$, $Cu(NO_3)_2.3H_2O$, $C_6N_6FeK_3$, $LiClO_4$, $Mg(NO_3)_2.6H_2O$, $Cl_2MnO_8.xH_2O$, $Ni(NO_3)_2.6H_2O$), $Pb(NO_3)_2$, $SnCl_2.2H_2O$, $C_4H_6O_4Zn.2H_2O$

THF (Tetrahydrofuran) was distilled using interaction of some little sodium metal pieces and benzophenone. It was heated under reflux for several hours until the color of solvent turns deep blue.

For CL measurements, a stopped-flow injection system combined with photomultiplier tube (PMT) was used. All the working solutions to be tested were freshly prepared. Dilutions were done by using distilled water. Prepared all solutions were protected from light and stored in refrigerator.

2.2 Instrumentation

Optical studies (absorption and radiation/fluorescence) were carried out using UV-vis Spectrometer/ Specord S600 and Thermo Lumina Fluorescence Device. Attenuated Total Reflectance" (ATR) unit with Thermo Scientific Nicolet iS10FTIR spectrometer device was used for Fourier Transform Infrared (FTIR) spectra of the monomers. Nuclear Magnetic Resonance (NMR) spectra of the monomers were recorded by a Bruker DPX-400 Spectrometer in DMSO or $CDCI_3$. Tetramethylsilane is used as the internal standard to interpret the chemical shifts in ^{1}H and ^{13}C NMR spectra.

The melting points of the target monomers were determined with the help of "GALLENKAMP 220/240 V, 50/60 Hz, 50 W" device. High resolution mass spectra for monomers were taken with Water, Synapt HRMS instrument.

2.2.1 CL Measurements

Pro-K.2000 Rapid Kinetic System was used for CL measurements, and the intensity of the emitted light was measured by using a photomultiplier tube (PMT) in dark environment. The system shown in Figure 2.1 based on the principle of stopping flow suddenly because CL reactions are very fast. Two different syringes are used to transfer the samples to the system. The intensity of the light emitted by the combination of the samples transferred from the syringes to the cell in the system is measured with the help of PMT.

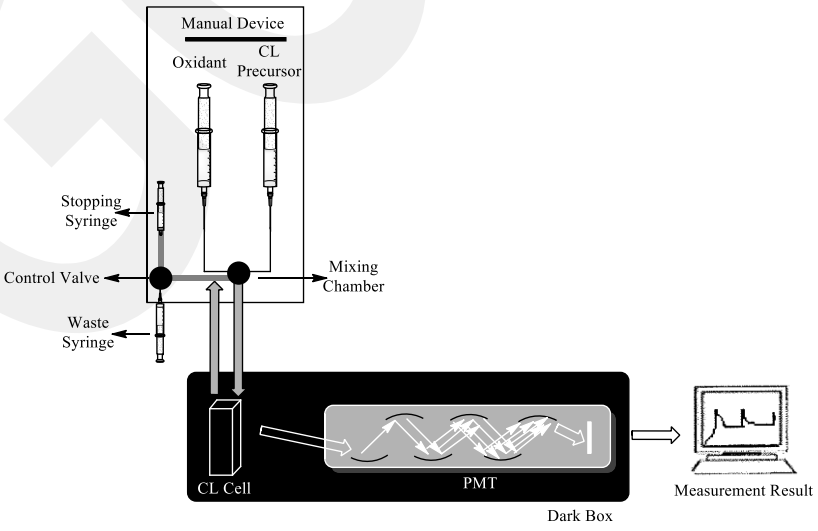

Figure 2.1 Schematic diagram for stopped-flow CL measurements

2.2.2 Electrochemical Measurements

Cyclic voltammetry technique was used to examine the electrochemical behavior of the compounds and the polymer (PS_2T-Lum). In cyclic voltammetry method, the current between the working electrode and the counter electrode is measured while the potential of the working electrode is scanned relative to the reference electrode. The voltammogram obtained as a result shows the potential against the current and gives information about the electroactivity and redox behavior of the substance. In addition, this method gives information about whether the mechanism of the electrochemical reaction is reversible and whether the formed product is subjected to reduction/oxidation processes again. In this study, cyclic voltammetry and electrolysis experiments were performed using Gamry PCI4/300 potentiostat-galvanostat device (Figure 2.2).

The polished platinum disc electrode is used as the working electrode (electrode area: 0.02 cm^2), and the platinum wire is used as the counter electrode. In addition, silver wire is used as a pseudo-reference (calibrated against 10 mM ferrocene/ferrocenium pair) or Ag/AgCl reference electrode in 1.0 M NaCl. To perform the detection of reactive oxygen species, indium tin oxide coated glass (ITO, Delta Tech. 8-12 Ω, 0.7 cm - 5 cm) is used as the working electrode, while Pt wire and silver wire are used as counter and reference electrodes, respectively. Ferrocene/ferrocenium redox couple was used as external standard (Ag/AgCl vs. $E_{Fc}+/F_c$ = 0.61 V).

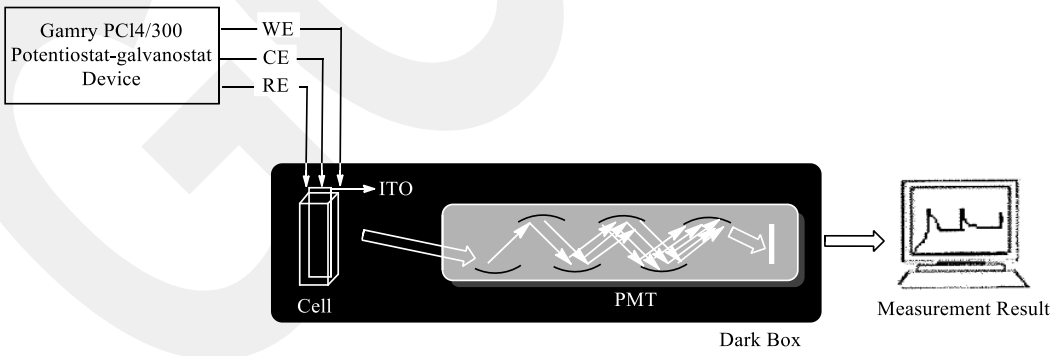

Figure 2.2 Schematic representation of electrolysis combined with PMT system

2.3 Synthesis of Monomers

2.3.1 Synthesis of F_2-PA (4,7-di(furan-2-yl)isobenzofuran-1,3-dione), S_2-PA (4,7-di(selenophen-2-yl)isobenzofuran-1,3-dione), F_2-PI-EtHex (2-(2-ethylhexyl)-4,7-di(furan-2-yl)isoindoline-1,3-dione), S_2-PI-EtHex (2-(2-ethylhexyl)-4,7-di(selenophen-2-yl)isoindoline-1,3-dione), and S_2-TPD-EtHex (5-(2-ethylhexyl)-1,3-di(selenophen-2-yl)-4H-thieno[3,4-c]pyrrole-4,6(5H)-dione) compounds

Firstly, 150 mg (0.49 mmol) of one of starting materials (compound 1 (3,6- dibromo phthalic anhydride), compound 2 (4,7-dibromo-2-(2-ethylhexyl) isoindoline-1,3-dione) or compound 3 (1,3-dibromo-5-(2-ethylhexyl)-4H-thieno[3,4-c]pyrrole-4,6(5H)-dione)) in 4 ml distilled THF is refluxed for half an hour under Ar atmosphere. Then 453.3 mg (1.079 mmol) of compound 4 (2-tributylstannyl furan) for furan-based structures or compound 5 (2-tributylstannyl selenophene) for selenophene based structures in 2 ml distilled THF is added at 60 ℃. After 30 minutes, 37.87mg (0.05 mmol) of bis(triphenylphosphine) palladium (II) dichloride, which is %5 of compound 4 and 5, in 4 ml distilled THF is added into the solution at 75 ℃. The reaction continues for 2 days under Ar atmosphere at 75 ℃. The reaction followed by thin layer chromatography (TLC) is finished and the reaction mixture is cooled to room temperature (Figure 2.3).

Water must not be added to the reaction medium, and extraction must not perform for materials contain phthalic anhydride unit as an acceptor (F_2-PA and S_2-PA). These compounds are purified by using a column chromatography with hexane and ethyl acetate as eluent. The purification is started with just hexane then switch to appropriate hexane: ethyl acetate mixture. Then, it is washed with hexane.

F_2-PI-EtHex, S_2-PI-EtHex and S_2-TPD-EtHex are purified by extraction method with water and DCM, then by column chromatography with hexane and ethyl acetate. The purification is started with just hexane, then switch to appropriate hexane: ethyl acetate mixture.

Compound F_2-PA: Yield: 80%, m.p.:160 ± 0.1 ºC. ^{1}H NMR (400 MHz, $CDCl_3$, δ, ppm): 8.40 (s, 2H, ArH); 8.00 (d, J=4 Hz, 2H, ArH); 7.65 (d, 2H, ArH); 6.67 (t, J=4 Hz, 2H, ArH) (Figure A.1). ^{13}C NMR (100 MHz, $CDCl_3$, δ, ppm): 162.04, 147.55, 144.09, 132.97,128.79, 124.01, 115.95, 112.86 (Figure A.2). FTIR (cm^{-1}): 3145, 1822, 1759, 1758, 1500, 1397, 1230, 1166, 1083, 1016, 930, 827, 736, 662 (Figure B.1). HRMS calculated for $C_{16}H_8O_5$, $[M+H]^+$: 281.045. Found for $C_{16}H_8O_5$, $[M+H]^+$: 281.045 (Figure C.1).

Compound S_2-PA: Yield: 60.0%, m.p.:197.5 ± 0.1 ºC. ^{1}H NMR (400 MHz, $CDCl_3$, δ, ppm): 8.29 (d, J=8 Hz, 2H, ArH); 8.00 (d, J=4 Hz, 2H, ArH); 7.92 (s, 2H, ArH); 7.47 (t, J=4 Hz, 2H, ArH) (Figure A.3). ^{13}C NMR (100 MHz, $CDCl_3$, δ, ppm): 161.86, 141.27, 137.56, 136.23, 134.83, 132.76, 130.49, 126.02 (Figure A.4). FTIR (cm^{-1}): 2361, 1818, 1763, 1614, 1546, 1477, 1363, 1220, 1159, 1078, 935, 833, 792, 745, 703, 641 (Figure B.2). HRMS calculated for $C_{16}H_8O_3Se_2$, $[M+H]^+$: 406.8890. Found for $C_{16}H_8O_3Se_2$, $[M+H]^+$: 406.8900 (Figure C.2).

Compound F_2-PI-EtHex: Yield: 45.2%, m.p.: decomposed. ^{1}H NMR (400 MHz, $CDCl_3$, δ, ppm): 8.22 (s, 2H, ArH); 7.98 (d, J=4 Hz, 2H, ArH); 7.60 (d, J=4 Hz, 2H, ArH); 6.61 (t, J=4 Hz, 2H, ArH), 3.64(d, J=8 Hz, 2H, -CH_2), 1.87-1.90 (m, 1H, -CH), 1.62-1.69 (m, 2H, -CH_2), 1.31-1.41 (m, 6H, -CH_2), 0.91-0.96 (m, 6H, -CH_3) (Figure A.5). ^{13}C NMR (100 MHz, $CDCl_3$, δ, ppm): 167.63, 148.64, 143.20, 131.59, 127.09, 125.54, 114.94, 112.33, 41.98, 38.11, 30.40, 28.13, 23.80, 22.83, 13.87, 10.21 (Figure A.6). FTIR (cm^{-1}): 2926, 2857, 1708, 1462, 1404, 1266, 1123, 1071, 910, 824, 743 (Figure B.1).

Compound S_2- PI-EtHex: Yield: 49.6%, m.p.:55 ± 0.1 ºC. ^{1}H NMR (400 MHz, $CDCl_3$, δ, ppm): 8.22 (d, J=4 Hz, 2H, ArH); 7.90 (d, J=4 Hz, 2H, ArH); 7.75 (s, 2H, ArH); 7.43 (t, J=4 Hz, 2H, ArH); 3.60 (d, J=8 Hz, 2H, -CH_2); 1.85-1.88 (m, 1H, -CH); 1.28-1.37 (m, 8H, -CH_2); 0.88-0.93 (m, 6H, -CH_3) (Figure A.7). ^{13}C NMR (100 MHz, $CDCl_3$, δ, ppm): 167.57, 142.67, 135.97, 134.23, 133.66, 131.93, 129.92, 127.09, 42.04, 38.0, 30.44, 28.40, 23.76, 22,93, 13.96, 10.33 (Figure A.8). FTIR (cm^{-1}): 3101, 2925, 2864, 1763, 1696, 1444, 1404, 1363, 1213, 1078, 820, 758, 697, 602 (Figure B.2). HRMS calculated for $C_{24}H_{25}NO_2Se_2$, $[M+H]^+$: 518.0302. Found for $C_{24}H_{25}NO_2Se_2$, $[M+H]^+$: 518.0301 (Figure C.3).

Compound S_2-TPD-EtHex: Yield: 87.0%, m.p: 130-132 °C. ^{1}H NMR (400 MHz, $CDCl_3$, ppm): 8.12 (d, J=5.6 Hz, 2H, ArH), 7.84 (d, J=3.8 Hz, 2H, ArH), 7.24 (t, J=5.5 Hz, 2H, ArH), 3.46 (d, J=7.3 Hz, 2H, -CH_2), 1.73-1.82 (m, 1H, -CH), 1.51-1.62 (m, 2H, CH_2), 1.18-1.31 (m, 6H, CH_2), 0.79-0.86 (m, 6H, -CH_3); ^{13}C NMR (100 MHz, $CDCl_3$, ppm) 163.2,138.9, 136.5, 135.7, 131.7, 130.3, 127.8, 42.5, 38.2, 30.6, 28.5, 23.9,23.1, 14.1, 10.5. FTIR (cm^{-1}): 3091, 2954, 2919, 2856, 1228, 1676, 1555, 1429, 1389, 1217, 1067, 937, 747, 690, 621 (Figure B.3) HRMS calculated for $C_{22}H_{23}NO_2SSe_2$, [M+H]+: 525.9858. Found for $C_{22}H_{23}NO_2SSe_2$, [M+H]+: 525.9868.

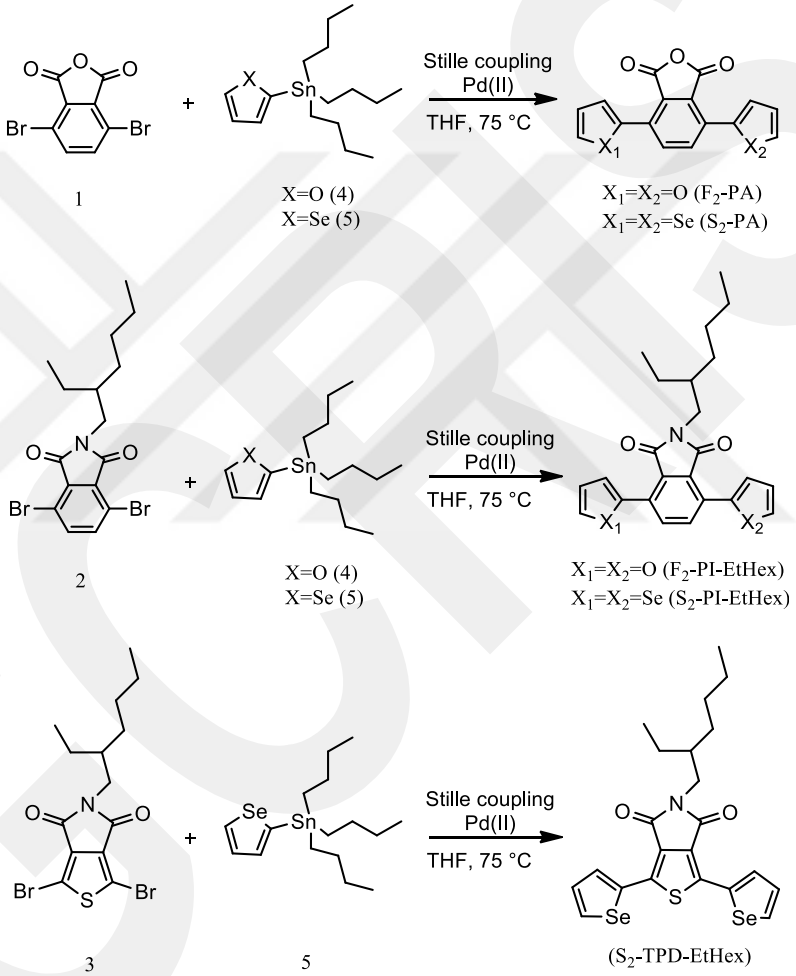

Figure 2.3 Synthesis ways to synthesize F_2-PA, S_2-PA, F_2-PI-EtHex, S_2-PI-EtHex and S_2-TPD-EtHex compounds

2.3.2 Synthesis of F_2B-Lum (5,8-di(furan-2-yl)-2,3-dihydrophthalazine-1,4-dione), S_2B-Lum (5,8-di(selenophene-2-yl)-2,3-dihydrophthalazine-1,4-dione) and S_2T-Lum (5,7-di(selenophen-2-yl)-2,3-dihydrothieno[3,4-d]pyridazine-1,4-dione)

i. Method 1

100 mg of F_2-PA or S_2-PA and 2 ml hydrazinium hydroxide were refluxed at 120 °C for 1 day in 2 ml glacial acetic acid. Then, it was cooled to room temperature and added water. After 1 day in the refrigerator, the precipitate formed is washed with 50 ml of water followed by 50 ml of hexane. Finally, it was dried under vacuum (Figure 2.4).

ii. Method 2

100 mg of F_2-PI-EtHex or S_2-PI-EtHex and 2 ml hydrazinium hydroxide were refluxed at 100 °C for 2 days in ethanol and 1,4-dioxane (3.5 mL, v/v). Then, it was cooled to room temperature and added water. After it was stored in the refrigerator for 1 day, the precipitate formed is washed with 50 ml of water followed by 50 ml of hexane. Finally, it was dried under vacuum (Figure 2.4).

100 mg of S_2-TPD-EtHex and 0.355 ml hydrazinium hydroxide were refluxed at 100 °C for 2 days in ethanol and 1,4-dioxane (3.5 mL, v/v). After it was stored in the refrigerator for 1 day, the precipitate formed is filtered and washed with 50 ml of ethanol and 1,4-dioxane (v/v) mixture followed by 50 ml of hexane. Finally, it was dried under vacuum (Figure 2.4).

Compound F_2B-Lum: Yield: 82.5% (from method 2); m.p.:134.7 ± 0,1 °C. ^{1}H NMR (400 MHz, DMSO, δ, ppm): 12.66 (s, 2H, ArH), 8.22 (s, 2H, ArH); 7.94 (d, J=4 Hz, 2H, ArH); 7.89 (d, J=4 Hz, 2H, ArH); 6.75 (t, J=4 Hz, 2H, ArH) (Figure A.9). ^{13}C NMR (100 MHz, DMSO, δ, ppm): 166.02, 148.34, 144.87, 131.88, 126.44, 124.49, 115.06, 112.92 (Figure A.10). FTIR (cm^{-1}): 3345, 3242, 3147, 1763, 1704, 1603, 1504, 1486, 1417, 1235, 1194, 1161, 1111, 1012, 950, 909, 834, 752, 670 (Figure B.1). HRMS calculated for $C_{16}H_{10}N_2O_4$, [M+H]+: 295.0719. Found for $C_{16}H_{10}N_2O_4$, [M+H]+: 295.0718 (Figure C.4).

Compound S_2B-Lum: Yield: 67.0% (from method 1), 85.0% (from method 2), m.p:160 ± 0,1 ºC. ^{1}H NMR (400 MHz, DMSO, δ, ppm): 12.6 (s, 2H, ArH); 8.42 (d, J=8 Hz, 2H, ArH); 7.94 (d, J=4 Hz, 2H, ArH); 7.87 (s, 2H, ArH); 7.43 (t, J=4 Hz, 2H, ArH) (Figure A.11). ^{13}C NMR (100 MHz, DMSO, δ, ppm): 165.76, 142.26, 135.77, 135.29, 133.15, 132.15, 129.75, 125.16 (Figure A.12). FTIR (cm^{-1}): 3329, 1767, 1699, 1537, 1480, 1417, 1340, 1225, 1090, 985, 903, 871, 825, 688, 647 (Figure B.2). HRMS calculated for $C_{16}H_{10}N_2O_2Se_2$, $[M+H]^+$: 422.9151. Found for $C_{16}H_{10}O_2Se_2$, $[M+H]^+$: 422.9153 (Figure C.5).

Compound S_2T-Lum: Yield: 32.0%. ^{1}H NMR (400 MHz, DMSO, δ, ppm): 11.42 (s, 2H, ArH); 8.41 (d, J=8 Hz, 2H, ArH); 7.85 (s, 2H, ArH); 7.35 (s, 2H, ArH) (Figure A.13). ^{13}C NMR (100 MHz, DMSO, δ, ppm): 171.67, 156.97, 138.51, 136.52, 132.25, 129.75, 124.02 (Figure A.14). FTIR (cm^{-1}): 2989, 2886, 1646, 1490, 1387, 1290, 1226, 1180, 1123, 825, 784, 678, 616, 567 (Figure B.3). HRMS calculated for $C_{14}H_8N_2O_2SSe_2$, $[M+H]^+$: 428.8715. Found for $C_{14}H_8N_2O_2SSe_2$, $[M+H]^+$: 428.8719 (Figure C.6).

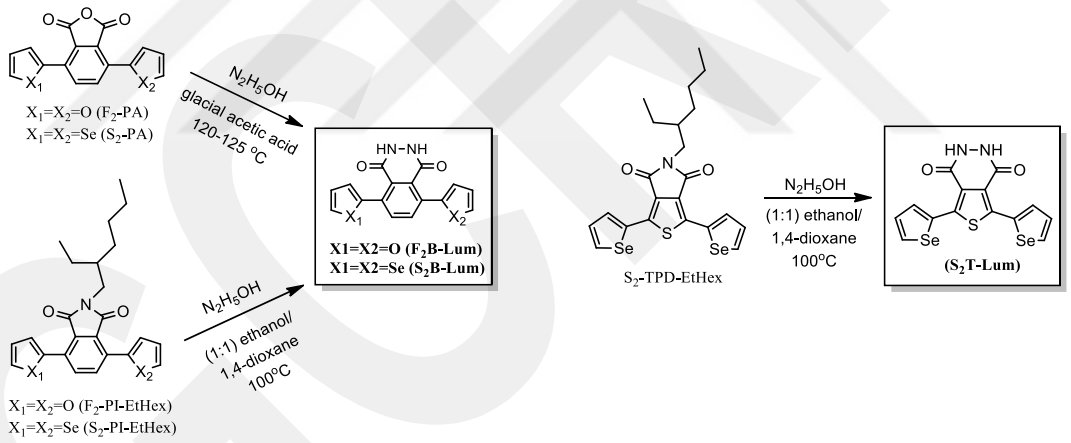

Figure 2.4 Synthesis ways to synthesize F_2B-Lum, S_2B-Lum and S_2T-Lum compounds

CHAPTER 3

RESULT AND DISCUSSION

F_2B-Lum, S_2B-Lum and S_2T-Lum were successfully synthesized in two steps using two different methods (see Figure 2.4). Compounds were usually obtained in orange and yellowish colors (Figure 3.1). Structural characterization of the compounds was performed by using NMR, FTIR and HRMS techniques. Phthalic anhydride-based compounds are sensitive to water. When they contact with water, their colors slowly turn from orange to black. For this reason, all experiments were carried out under argon atmosphere and the compounds were stored under argon gas in a refrigerator.

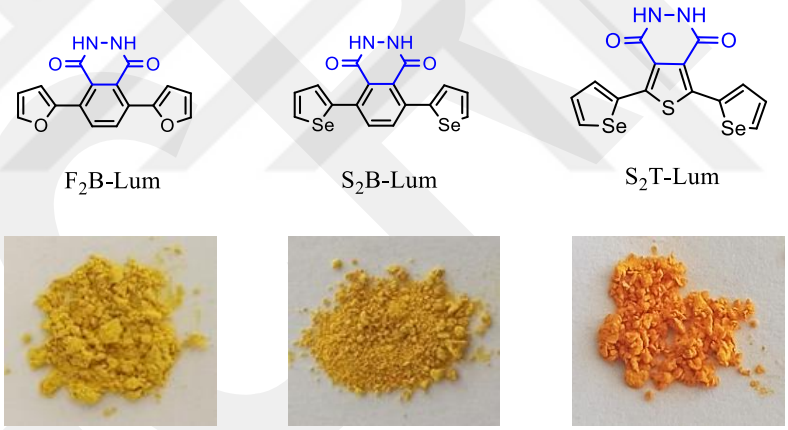

F_2B-Lum S_2B-Lum S_2T-Lum

Figure 3.1 Structures and pictures of the chemiluminescent compounds

^{1}H and ^{13}C NMR spectra of the molecules are given in Appendix A. For example, as a representative example, while a singlet signal observed at 8.22 ppm can be attributed to the protons of phenyl ring, the other signals (doublet signals at 7.94 and 7.89 ppm and a doublet of doublet signal at 6.74 ppm) belong to protons of furan rings in the ^{1}H NMR spectrum of F_2B-Lum (Figure A.9). On the other hand, as expected, 8 different carbon signals can be easily observed in the ^{13}C NMR spectrum of F_2B-Lum (Figure A.10).

In the ^{1}H NMR spectrum of S_2T-Lum (Figure A.13), protons of –NH- groups can be seen as a broad signal centered at 11.42 ppm and the peaks between 8.5 ppm and 7.25 ppm are ascribed to the protons of selenophene rings.

The FTIR spectra of the compounds were taken and compared with each other in Appendix B. The peaks around 690 cm^{-1} and 745 cm^{-1} belongs to selenophene and furan rings, respectively. The carbonyl groups (C=O) connected to N revealed a peak around 1700 cm^{-1} and connected to O revealed a peak around 1760 cm^{-1}. The peaks between 2850-2950 cm^{-1} indicate the alkyl groups so these signals can be found only in the FTIR spectra of compounds that contain ethyl-hexyl units (Figures B.1-B.3). The presence of the peaks around 2900-3300 cm^{-1} represents the N-H group in the FTIR spectra of the luminol-type structures (F_2B-Lum, S_2B-Lum and S_2T-Lum) [65]. Finally, the values found experimentally in HRMS spectra of all compounds are absolutely compatible with their theoretical values (Figures C.1-C.6).

3.1 Optical Properties

The optical properties of the compounds were examined in DMSO in Figure 3.2. While in the short wavelength peaks (around 265 nm) belong to π- π * the transition band, the long wavelength peaks (around 330 nm) indicate the charge transfer between A and D units. While F_2B-Lum, S_2B-Lum and luminol represent two main absorption bands, but S_2T-Lum has three absorption bands, which can be due to the presence of the difference acceptor units (benzene and thiophene). Like absorption spectrum, a similar behavior was observed in the fluorescence spectra. As seen in Figure 3.2, luminol emits at 400 nm, and F_2B-Lum and S_2B-Lum emit around 440 nm. On the other hand, an emission band at 523 nm was observed for S_2T-Lum. Due to the D-A-D structure, the compounds have longer conjugation when compared to luminol, which results in a longer wavelength emission. While F_2B-Lum and S_2B-Lum emit greenish blue, S_2T-Lum emits green. All absorption and emission bands of the compounds are listed in the Table 3.1.

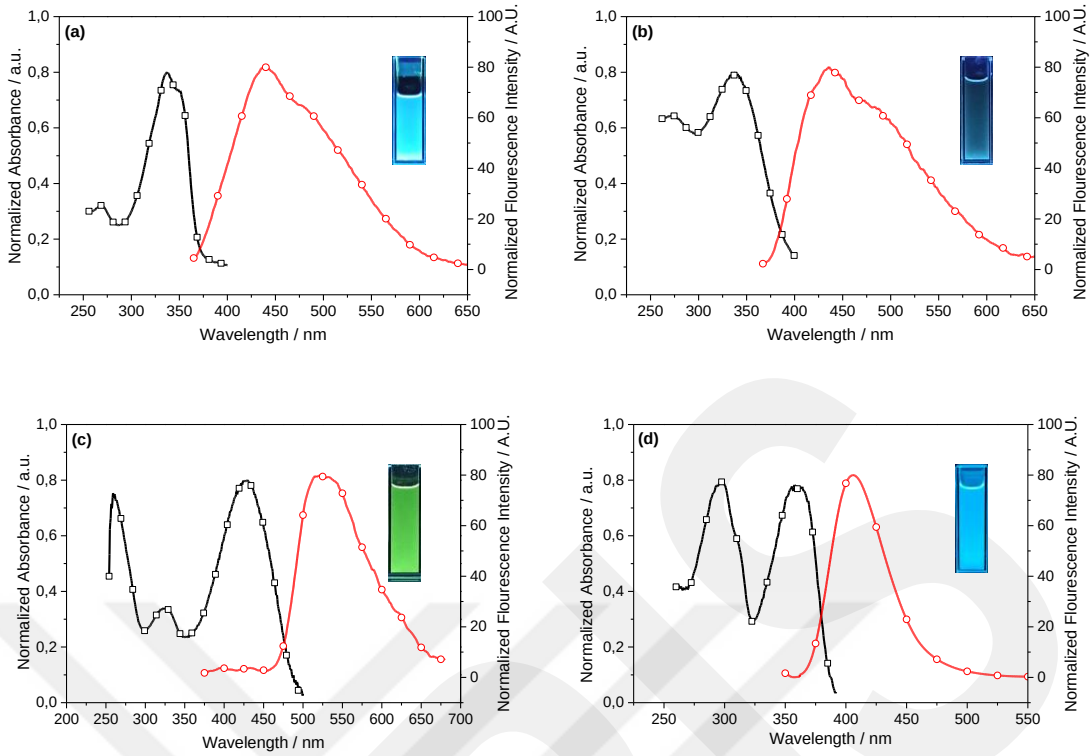

Figure 3.2 Comparative absorption (black line/square) and emission (red line/circle) spectra of (a) F_2B-Lum, (b) S_2B-Lum, (c) S_2T-Lum and (d) luminol (solvent: DMSO), inside pictures: Emission of compounds under UV lamp (365 nm)

Table 3.1 Absorption and emission bands of F_2B-Lum, S_2B-Lum, S_2T-Lum and luminol (solvent: DMSO)

Compound	Absorption (nm)	Emission (nm)
F_2B-Lum	272, 337	425.3
S_2B-Lum	277, 342.5	422
S_2T-Lum	259, 324.5, 429	523
Luminol	298, 357.5	406.1

3.2 Quantum Yield (QY)

The following equation is used to calculate the quantum yields of the compounds. [66]:

$$QY_{sample} = QY_{standard} \times \left(\frac{F_{sample}}{F_{standard}}\right) \times \left(\frac{A_{standard}}{A_{sample}}\right) \times \left(\frac{n_{sample}}{n_{standard}}\right)^2 \quad (1.12)$$

n = refractive index of the solvent

A = absorption value at the wavelength at which the excitation is made

F = area of the emission spectrum obtained

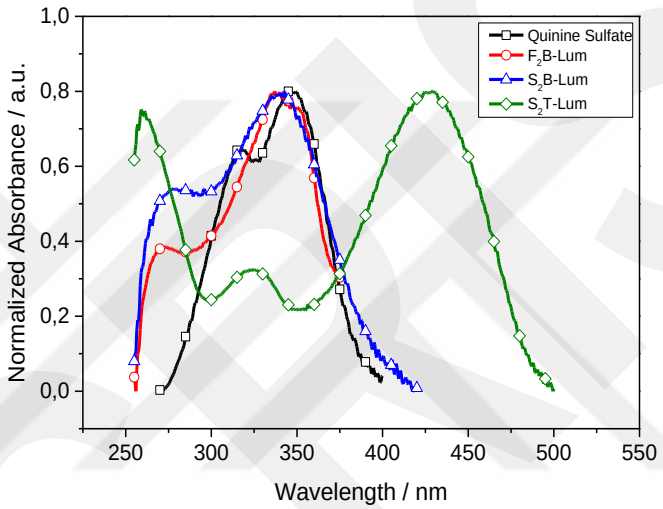

Figure 3.3 Absorption spectra of quinine sulfate (in 0.1 M H_2SO_4(aq)), F_2B-Lum, S_2B-Lum and S_2T-Lum (in DMSO) ($\lambda_{excitation}$ = 350 nm)

In order to measure the quantum yield of the compounds, the quinine sulfate standard (QY=58% at 22 ^oC in 0.1 M H_2SO_4(aq)) was chosen because the absorption spectrum was very compatible with the chemiluminescent compounds. 0.1 M H_2SO_4(aq) was used as a solvent for the standard and DMSO were used for the samples. The results obtained are given in Table 3.2. In order to calculate the quantum yields of compounds with respect to luminol, the quantum yield of luminol was taken as 100%. As seen in Table 3.3, F_2B-Lum, S_2B-Lum and S_2T-Lum compounds have lower quantum efficiency compared to luminol. The solvent has a great influence on this situation. Another factor is that the resonance effect in the D-A-D system is limited due to the steric effect between the D and A units and the magnitude of the dihedral angle. The dihedral angle disrupts the planarity [67-68].

Table 3.2 Quantum yields of the compounds obtained in DMSO ($\lambda_{excitation}$ = 350 nm). Quinine Sulfate Standard (in 0.1 M H_2SO_4(aq)) QY = 58% [69]

Compounds	**QY**
F_2B-Lum	0.12
S_2B-Lum	0.07
S_2T-Lum	0.34
Luminol	17.63

Table 3.3 Quantum yields ($\lambda_{excitation}$ = 350 nm) of compounds with respect to luminol (considering the luminol quantum yield as 100%)

Compound	**QY**
F_2B-Lum	0.68
S_2B-Lum	0.40
S_2T-Lum	1.93
Luminol	100

3.3 CL Properties

The CL properties of F_2B-Lum, S_2B-Lum and S_2T-Lum were investigated and compared to luminol. The system shown in Figure 2.1 was used to examine the CL properties. One of the syringes in the system contains hydrogen peroxide and a metal cation, while the other contains CL material dissolved in NaOH(aq). For blood and hemin measurements, one syringe contains blood or hemin solution with the CL precursor, while the other contains only hydrogen peroxide solution.

H_2O_2 as an oxidant, metal cations or blood or hemin as a catalyst were used to measure CL properties of CL compounds in alkaline solution. While taking measurements, 10^{-6} M of the compounds, 10^{-3} M of H_2O_2 and 10^{-3} M of metal cations were used. Blood and hemin were diluted in different proportions by volume using water. The compounds and hemin solutions were prepared in 0.1 M NaOH(aq) solution. H_2O_2, metal cations and blood solutions were prepared in distilled water.

Firstly, in order to reveal the CL property of the compounds, CL radiation was investigated with different oxidants in basic environment. $KMnO_4$, $K_2Cr_2O_7$ and H_2O_2 were used as oxidants. When the CL radiation intensities of different oxidants prepared at the same concentration were compared, it was observed that H_2O_2 was very effective (Figure 3.4).

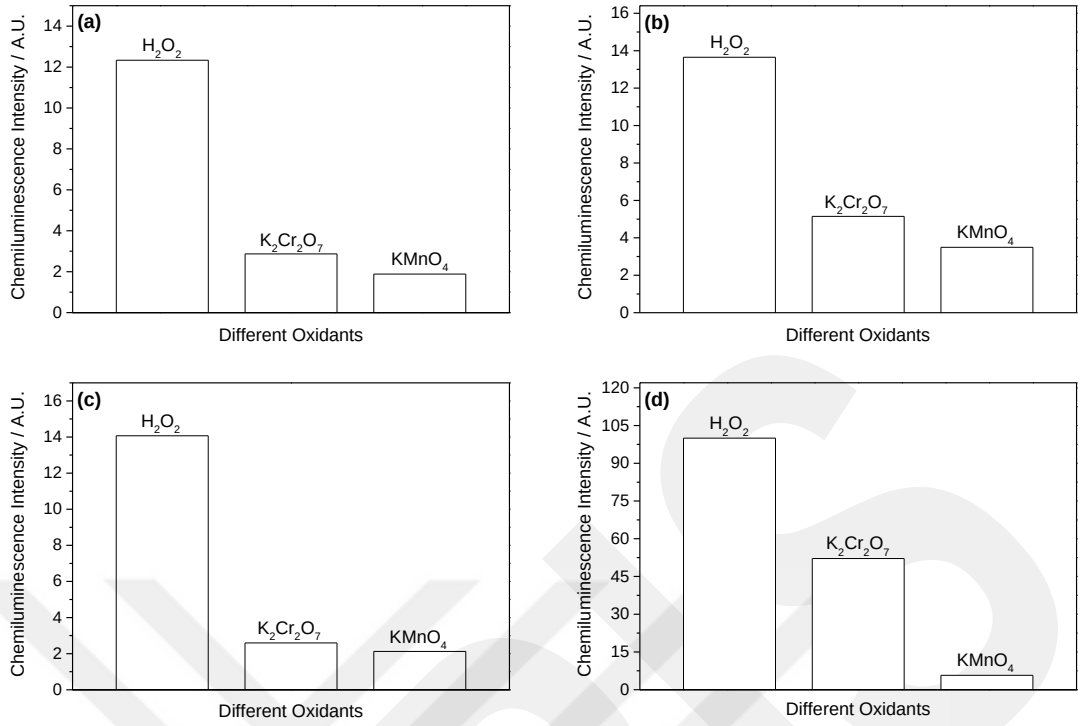

Figure 3.4 The CL intensity of 1.0×10^{-6} M (a) F_2B-Lum, (b) S_2B-Lum, (c) S_2T-Lum and (d) luminol in 0.1 M NaOH(aq) with 10^{-3} M of various oxidants

The compounds contain the same CL unit with luminol in their structure. So, by inspiring from CL mechanism of luminol, a similar mechanism was proposed in Figure 3.5 for F_2B-Lum, S_2B-Lum and S_2T-Lum. According to the mechanism, the compound interacts with an oxidizing agent such as hydrogen peroxide in an alkaline medium. Then, a bridge is formed by peroxides between the carbonyl groups in the pyridazine ring. This bridge stretches the existing ring and causes it to break irreversibly. Finally, it gives the energy in the form of light. As a result, a blue-green light is observed.

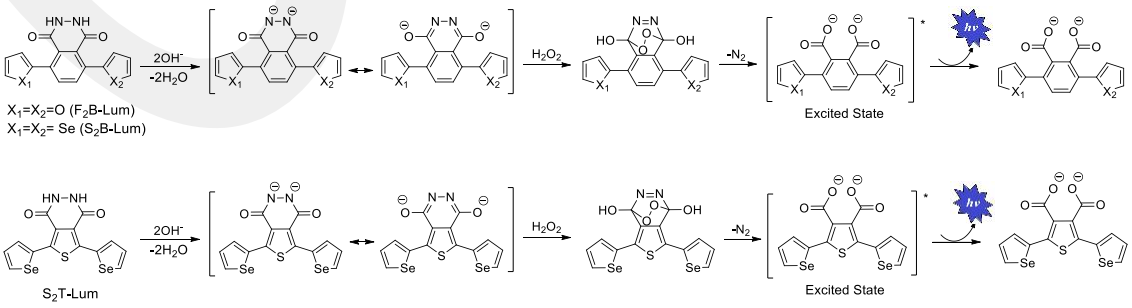

Figure 3.5 A proposed mechanism for the CL compounds

Figure 3.6 shows the CL radiation intensity of the compounds which react with different hydrogen peroxide concentrations in basic medium. According to Figure 3.6, the CL light intensity increases as a function of hydrogen peroxide concentration. Also, even when hydrogen peroxide is at a very low concentration, the CL radiation intensity of the compounds can be measured.

Hydrogen peroxide can be life threatening if it presents in the body at levels of $5x10^{-5}$ M and above [70]. The compounds exhibit sensitivity up to $1.0x10^{-6}$ M hydrogen peroxide levels. Thus, it is possible to use them in sensor studies to determine the amount of hydrogen peroxide in the body.

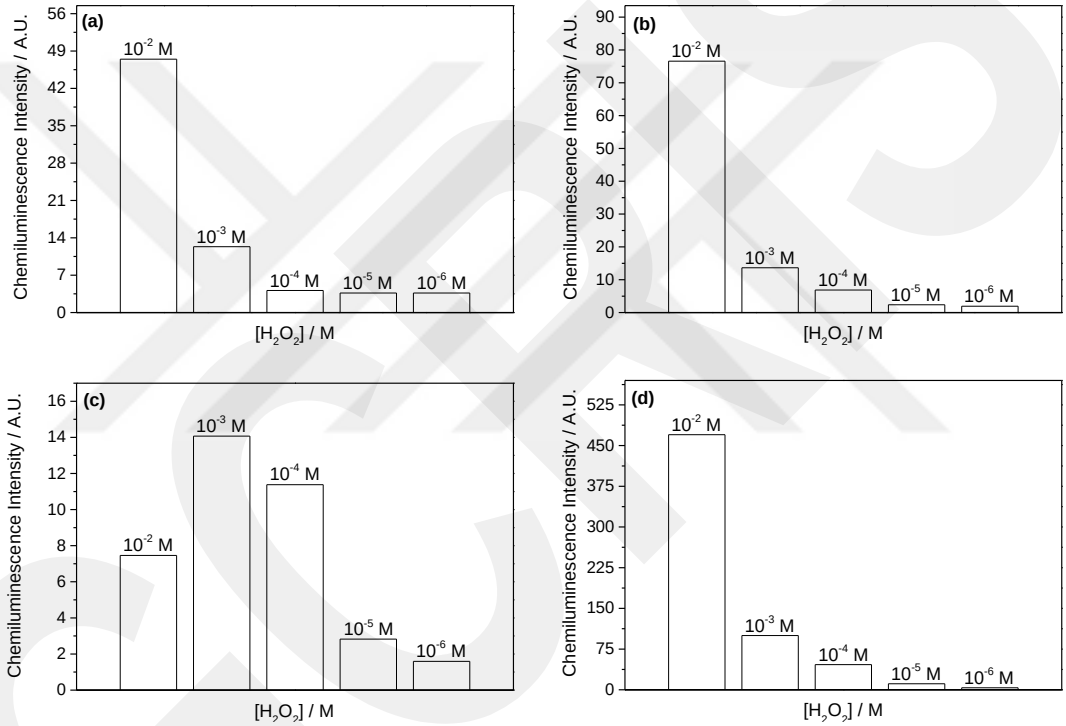

Figure 3.6 The CL intensity of 1.0×10^{-6} M (a) F_2B-Lum, (b) S_2B-Lum, (c) S_2T-Lum and (d) luminol in 0.1 M NaOH(aq) with different H_2O_2 concentrations

After determining that the compounds can react with hydrogen peroxide and emit light, it was checked whether the metal ion could catalyze this radiation. In order to be used in forensic science applications, the behavior of CL reaction in the presence of Fe^{3+} ion is important. Therefore, the effect of Fe^{3+} ion as a catalyst in the reaction was investigated. Figure 3.7 shows the CL emission of the compounds with H_2O_2 in the presence (red line (ii)) and absence (black line (i)) of catalyst in a basic medium.

As can be seen in Figure 3.7(i), while CL intensities are very low and pale in the absence of Fe^{3+} ion, the light intensity increases sharply in the presence of Fe^{3+} ion, which confirms the catalytic effect of Fe^{3+} ions on CL reaction.

In addition, while iron ion increased the emission of luminol by 10.5 times, it increased the emission of F_2B-Lum, S_2B-Lum and S_2T-Lum approximately 4.12, 20.8 and 2.2 times, respectively. According to this result, it can be concluded that Fe^{3+} ion can catalyze the CL reaction of S_2B-Lum much more than luminol.

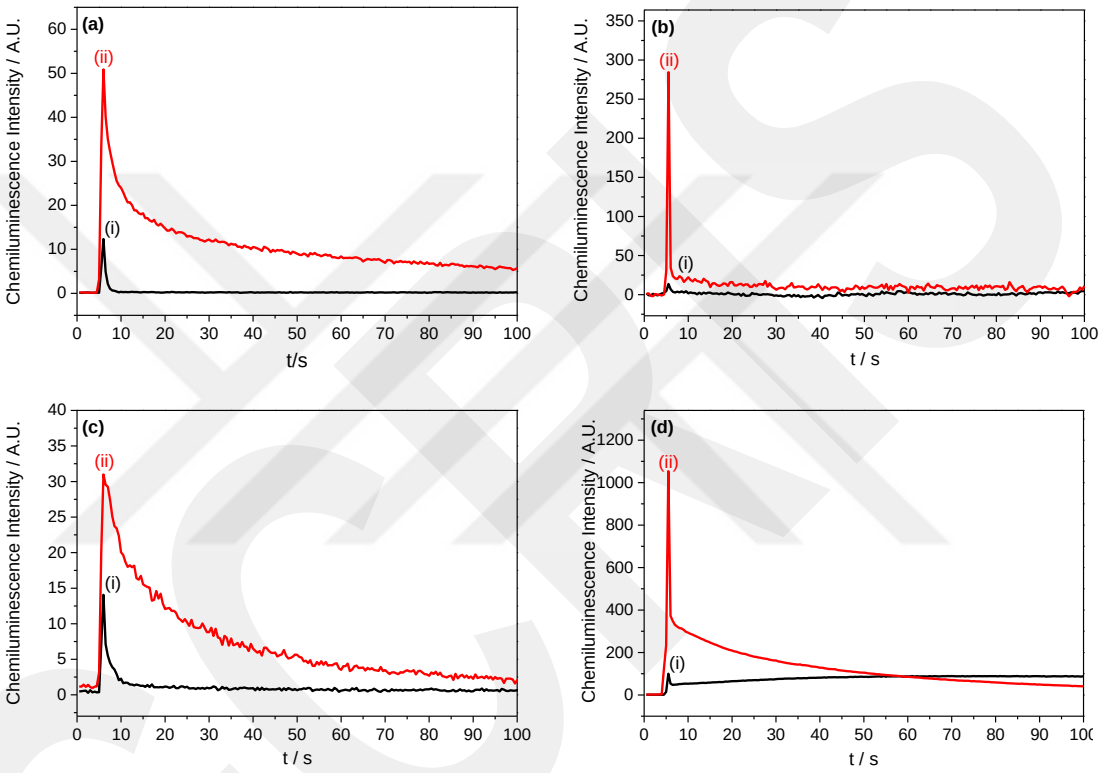

Figure 3.7 The CL intensity of 1.0×10^{-6} M (a) F_2B-Lum, (b) S_2B-Lum, (c) S_2T-Lum and (d) luminol in 0.1 M NaOH(aq) with 1.0×10^{-3} M H_2O_2 (i) in the absence and (ii) in the presence of 1.0×10^{-3} M Fe^{3+} ion

In the presence of Fe^{3+} ion, the intensity increases sharply and then decreases, but in the presence of blood samples, the intensity seems to increase and then decrease slowly. Thus, the difference between iron and blood samples can be easily understood. For example, Figure 3.8 shows the CL intensity of S_2T-Lum compound in the absence and in the presence of blood sample diluted with water in 1 to 100,000 ratio.

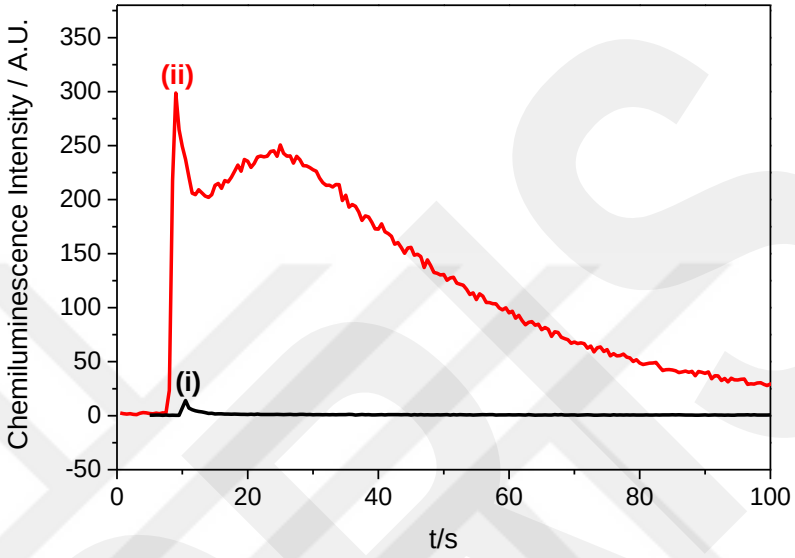

Figure 3.8 The CL intensity of 1.0×10^{-6} M S_2T-Lum with 1.0×10^{-3} M H_2O_2 in 0.1 M NaOH(aq) (i) in the absence and (ii) the presence of blood sample diluted with water in 1/100,000 ratio

To investigate the effect of different metal ions on the CL intensity of the compounds, the CL reaction was repeated with various metal ions (Figure 3.9). The same study was repeated with the luminol as a reference. In Figure 3.9, while the CL reaction of the compounds was catalyzed especially by copper and iron metal ions, the catalytic effect of other metal ions was very low. Therefore, the CL property of the compounds can be used in the field of analytical chemistry for the recognition and quantification of copper and iron metal ions. In addition, the compounds can facilitate the detection of hydrogen peroxide, as the presence of metal ions greatly increases CL radiation. Table 3.4 represents the coefficient of increase in CL intensity of $1.0\text{x}10^{-6}$ M of the compounds with $1.0\text{x}10^{-3}$ M H_2O_2 in 0.1 M NaOH(aq) in the presence of $1.0\text{x}10^{-3}$ M of different metal ions.

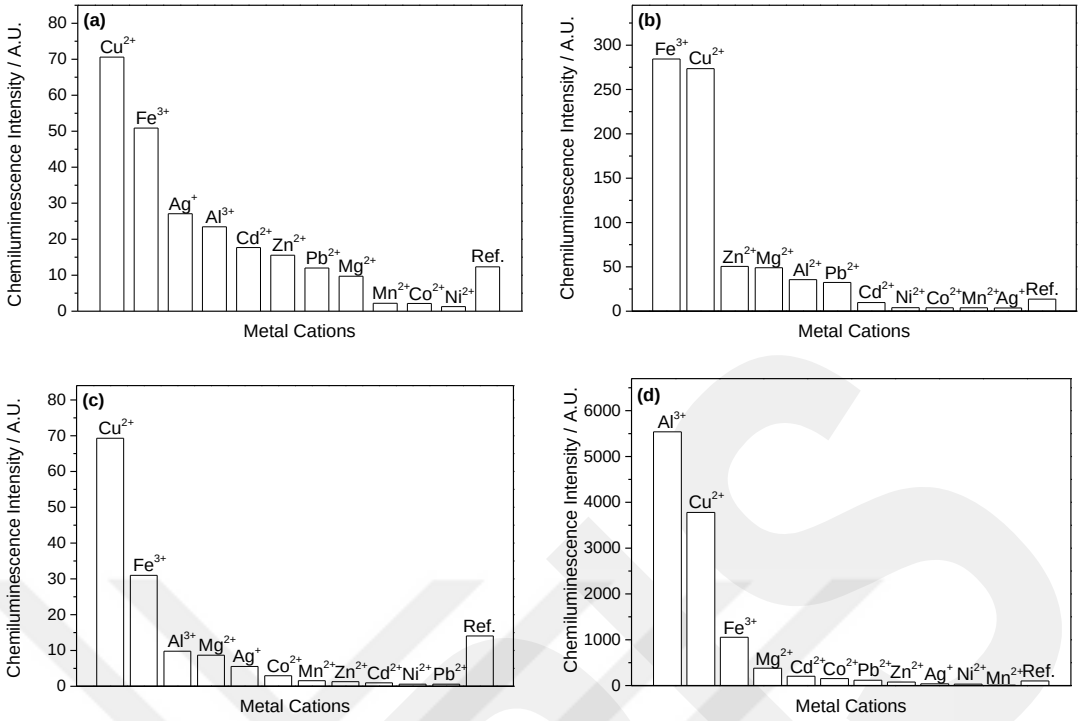

Figure 3.9 The CL intensity of 1.0×10^{-6} M of (a) F_2B-Lum, (b) S_2B-Lum, (c) S_2T-Lum and (d) luminol with 1.0×10^{-3} M H_2O_2 in 0.1 M NaOH(aq) in the presence of 1.0×10^{-3} M of different metal ions

Table 3.4 The coefficient of increase in CL intensity of 1.0×10^{-6} M of the compounds with 1.0×10^{-3} M H_2O_2 in 0.1 M NaOH(aq) in the presence of 1.0×10^{-3} M different metal ions

	Compounds			
	F_2B-Lum	**S_2B-Lum**	**S_2T-Lum**	**Luminol**
Ref	1	1	1	1
Ag^+	x2.2	x0.3	x0.4	x0.4
Al^{3+}	x1.9	x2.6	x0.7	x55.4
Cd^{2+}	x1.4	x0.7	x0.1	x2.0
Co^{2+}	x0.2	x0.3	x0.2	x1.5
Cu^{2+}	x5.7	x20.0	x4.9	x37.8
Fe^{3+}	x4.1	x20.8	x2.2	x10.5
Mg^{2+}	x0.8	x3.6	x0.6	x3.8
Mn^{2+}	x0.2	x0.3	x0.1	x0.1
Ni^{2+}	x0.1	x0.3	x0.1	x0.3
Pb^{2+}	x1.0	x2.4	x0.1	x1.2
Zn^{2+}	x1.3	x 3.7	x0.1	x0.8

As shown in Figure 3.7, the CL reaction of the compounds can be catalyzed in the presence of Fe^{3+} ions. The effect of Fe^{3+} ion concentration on this reaction is shown in Figure 3.10 using different Fe^{3+} ions. Thus, the potential use of the compounds in blood detection in forensic science will be understood. As seen in Figure 3.10, the CL intensity of the compounds were observed clearly in the presence of 10^{-3} M and more concentrated Fe^{3+} ions. Also, similar examination has been done for different Cu^{2+} ion concentrations too in Figure 3.11.

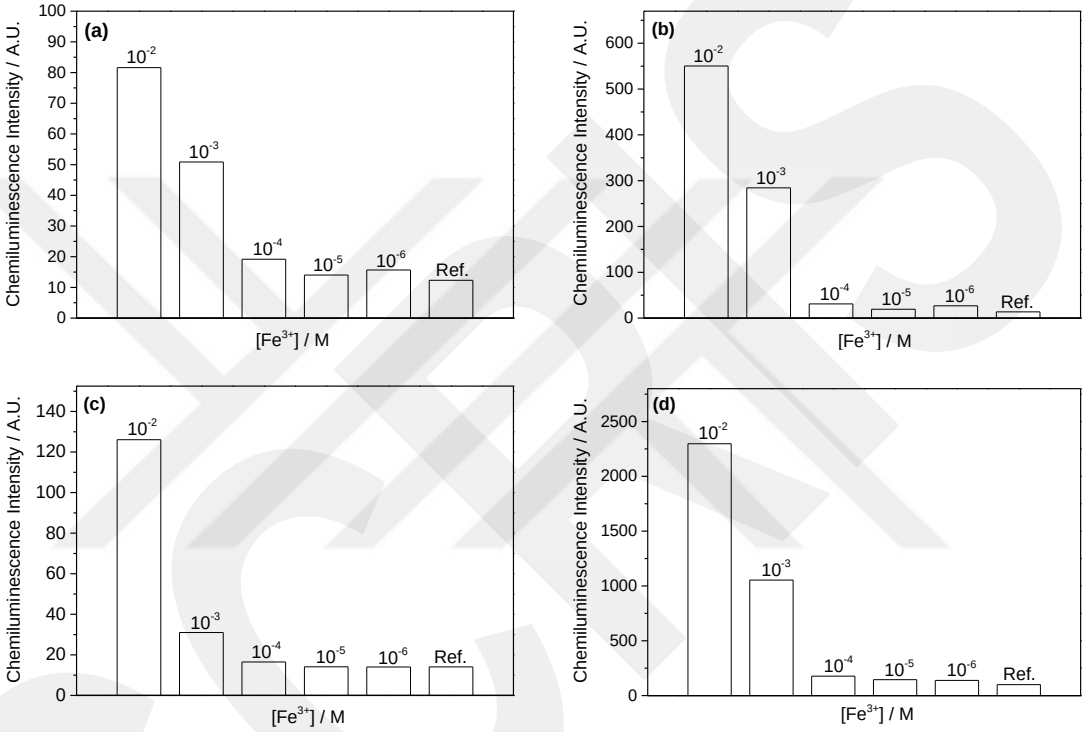

Figure 3.10 The CL intensity of 1.0×10^{-6} M of (a) F_2B-Lum, (b) S_2B-Lum, (c) S_2T-Lum and (d) luminol with 1.0×10^{-3} M H_2O_2 in 0.1 M NaOH(aq) in the presence of different Fe^{3+} ion concentrations

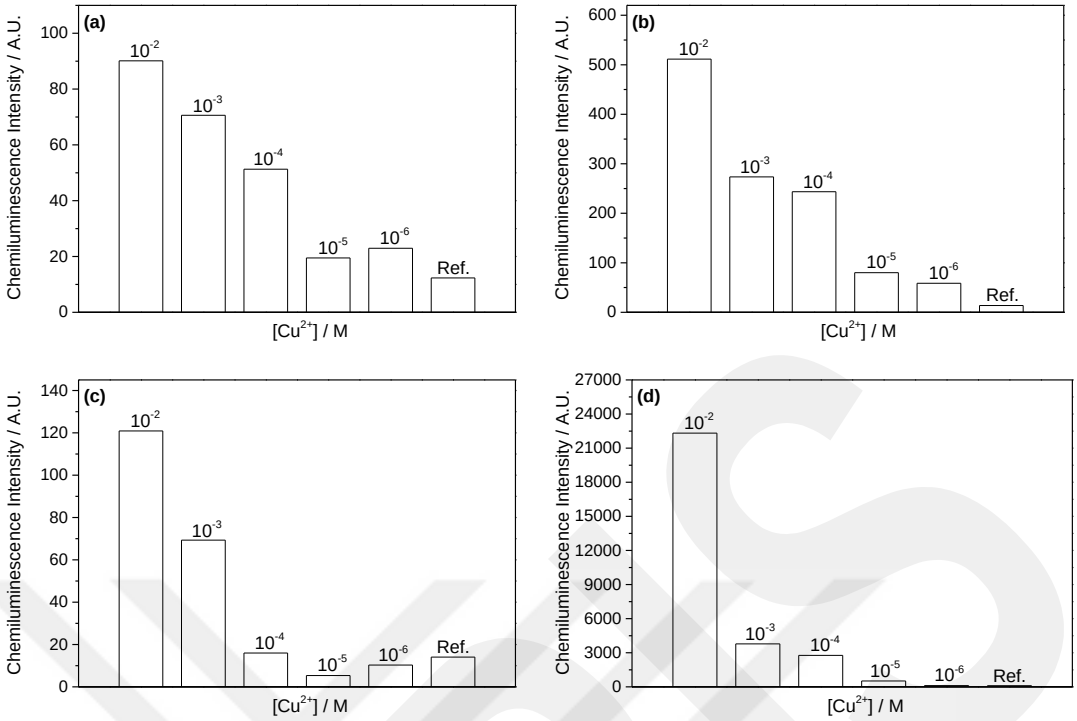

Figure 3.11 The CL intensity of 1.0×10^{-6} M of (a) F_2B-Lum, (b) S_2B-Lum, (c) S_2T-Lum and (d) luminol with 1.0×10^{-3} M H_2O_2 in 0.1 M NaOH(aq) in the presence of different Cu^{2+} ion concentrations

Like the Fe^{3+} ion, it is seen that the CL reaction of the compounds is catalyzed by hemin even up to a concentration of 10^{-6} M (Figure 3.12). The intensity obtained from the CL reactions of the compounds in the presence of hemin increased in direct proportion to the hemin concentration.

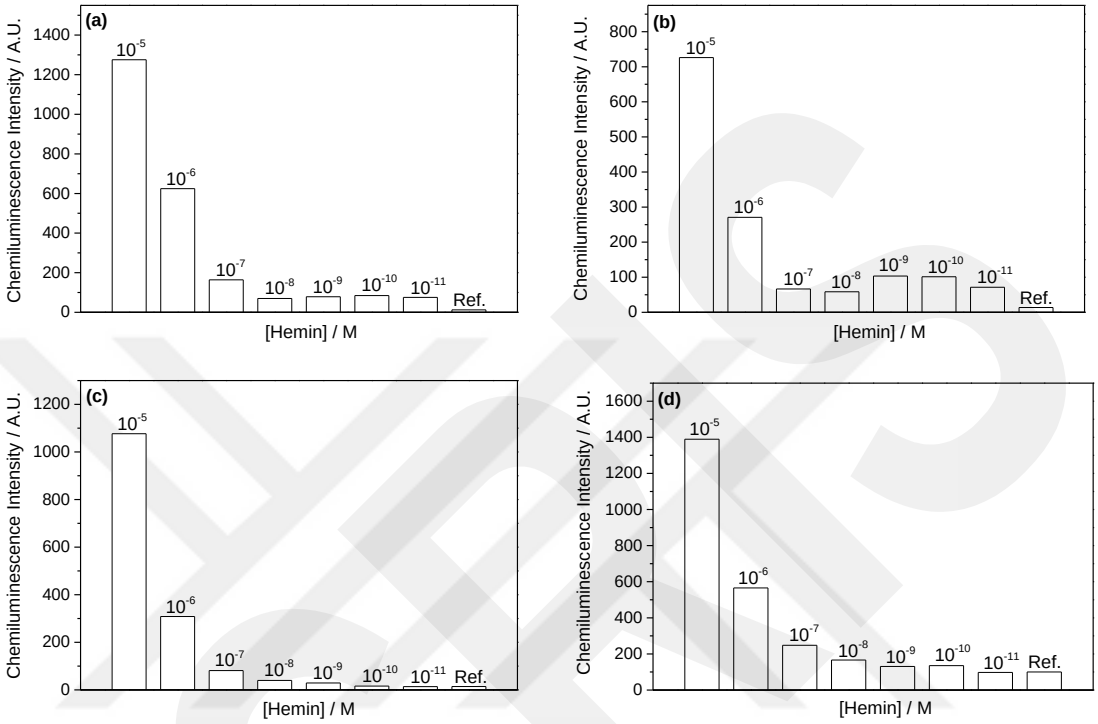

Figure 3.12 The CL intensity of 1.0×10^{-6} M of (a) F_2B-Lum, (b) S_2B-Lum, (c) S_2T-Lum and (d) luminol with 1.0×10^{-3} M H_2O_2 in 0.1 M NaOH(aq) in the presence of different hemin concentrations

Like the catalytic effect of hemin samples on the CL reaction of the compounds, a similar behavior was expected to be observed in blood samples. Therefore, the reaction was repeated with blood samples diluted with different proportions of water. The CL of the compounds was observed even in the dilution of blood at a rate of 1 to 100,000 for F_2B-Lum, at a rate of 1 to 1,000,000 for S_2B-Lum and at a rate of 1 to 1,000,000 for S_2T-Lum (Figure 3.13).

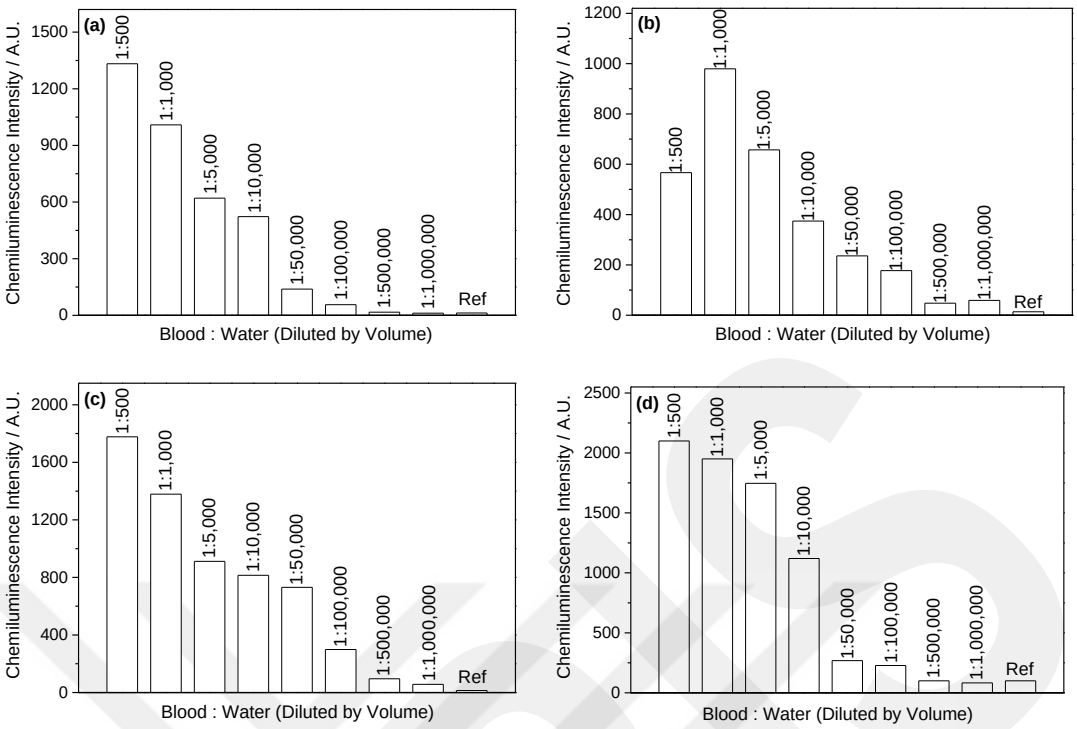

Figure 3.13 The CL intensity of 1.0×10^{-6} M of (a) F_2B-Lum, (b) S_2B-Lum, (c) S_2T-Lum and (d) luminol with 1.0×10^{-3} M H_2O_2 in 0.1 M NaOH(aq) in the presence of blood samples diluted with water in different ratios

Although blood detection was aimed in forensic medicine in this study due to the Fe^{3+} ion content of hemoglobin in the blood, it was observed that CL compounds were generally more sensitive to copper as a result of the analyzes. For this reason, in addition to iron, other metal ratios in the blood were also investigated. While copper in the blood is 0.131-0.132 mg per hundred cubic centimeters, the iron rate is 45.0-50.0 mg per hundred cubic centimeters. This means that the iron concentration in the blood is approximately 8.5×10^{-3} M. The amount of copper ion in the blood is 360 times less than the iron ion [71]. Concentrations of other metals in the blood are also traces compared to iron ions [72]. For this reason, iron ion sensitivity is great importance for blood detection.

3.4 Electrochemical Behaviors of F_2B-Lum and S_2B-Lum and Their Use in Reactive Oxygen Species Detection

In order to examine the redox behavior of the compounds, cyclic voltammetry method was used. In Figure 3.14(a), as a representative example, F_2B-Lum exhibits an irreversible oxidation signal at 1.83 V (V_{onset}=1.50 V) during anodic scanning. Unfortunately, F_2B-Lum couldn't be polymerized successfully via repeating cycles between 0.0 and 2.0 V. On the other hand, during a cathodic scan F_2B-Lum does not represent any reduction peak under inert atmosphere. It is well-known that dissolved oxygen species in the electrolyte solution can be reduced by applying an external potential of about -1.0 V to the working electrode under ambient conditions. Therefore, reactive oxygen species can be obtained, and they can attack a chemiluminescent compound in the medium. Under the light of this information, an experiment was performed for F_2B-Lum via square wave potential technique by applying 0.0 V and -1.05 V. As expected, reactive oxygen species were formed and they attacked to F_2B-Lum; therefore, the CL reaction was triggered. This reaction can be followed via PMT integrated to the electrolysis cell. Figure 3.14(b) represents the CL reaction of F_2B-Lum with reactive oxygen species created in the medium. A similar behavior was also observed for S_2B-Lum (see Figure 3.15). During anodic scan S_2B-Lum exhibited one irreversible oxidation signal at 1.64 V (V_{onset}= 1.37 V) with a shoulder at 1.06 V (Vonset=0.84 V) and unfortunately it couldn't also be polymerized.

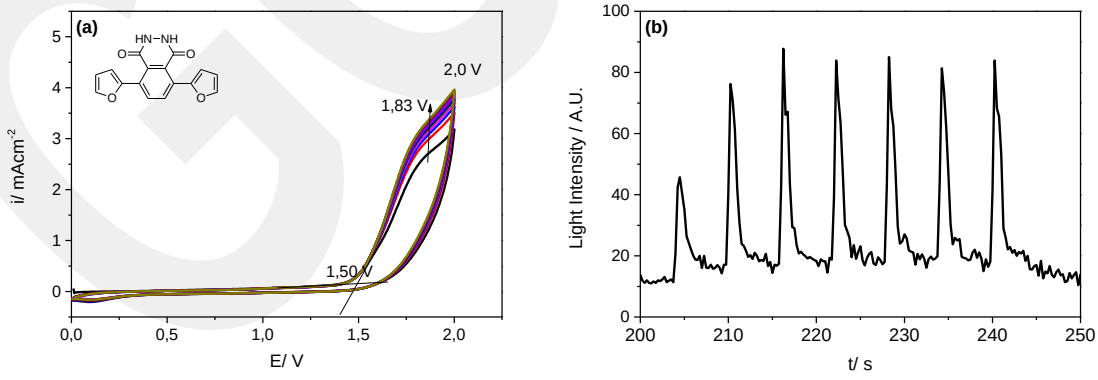

Figure 3.14 Cyclic voltammograms of F_2B-Lum on Pt electrode in 0.1 M TBAH/ACN electrolyte solution between 0.0 V and 2.0 V at a scan rate of 100 mV/s and under inert atmosphere (b) CL intensity of F_2B-Lum with reactive oxygen species formed via square wave potential method at -1.05 V (2 s) and 0.0 V (5 s) in 0.1 M TBAH/ACN electrolyte solution under ambient condition

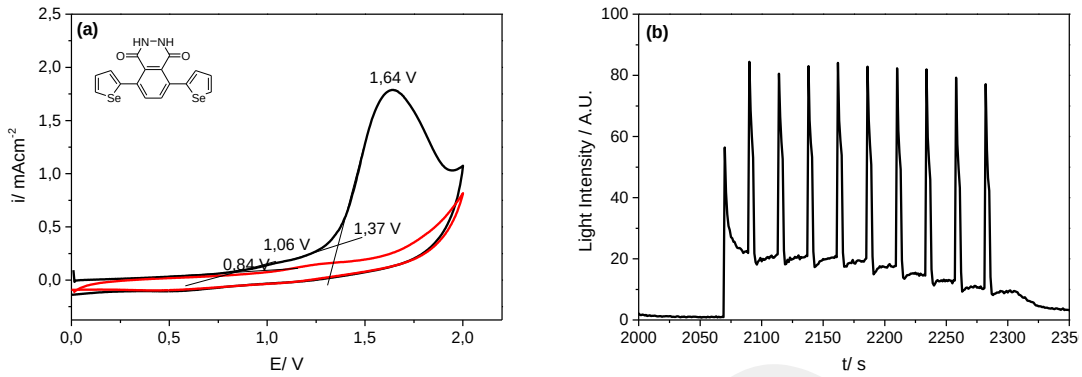

Figure 3.15 Cyclic voltammograms of S_2B-Lum on Pt electrode in 0.1 M TBAH/ACN electrolyte solution between 0.0 V and 2.0 V at a scan rate of 100 mV/s and under inert atmosphere (b) CL intensity of S_2B-Lum with reactive oxygen species formed via square wave potential method at -1.05 V (2 s) and 0.0 V (5 s) in 0.1 M TBAH/ACN electrolyte solution under ambient condition

3.5 Electropolymerization of S_2T-Lum

As seen in Figure 3.16, during anodic scan S_2T-Lum exhibited a well-defined irreversible oxidation signal at 1.28 V (V_{onset}=1.12 V), which is responsible from electropolymerization.

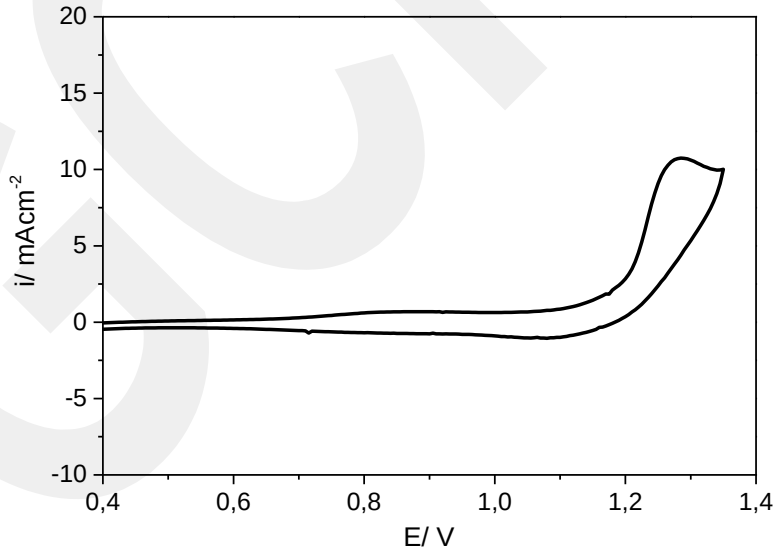

Figure 3.16 Cyclic voltammogram of S_2T-Lum on Pt electrode in 0.1 M TBAH/ACN-BF_3.Et_2O (95:5- v/v) electrolyte solution between 0.25 V and 1.3 V at a scan rate of 100 mV/s

Electrochemical polymerization was performed successfully via repeating cycles between 0.25 V and 1.35 V (see Figure 3.17). After the first cycle, a new redox couple appears and its current intensity increases as a function of cycle numbers, which confirms the formation of an electroactive polymer film (PS_2T-Lum) on the electrode surface and an increase in the film thickness after each cycle.

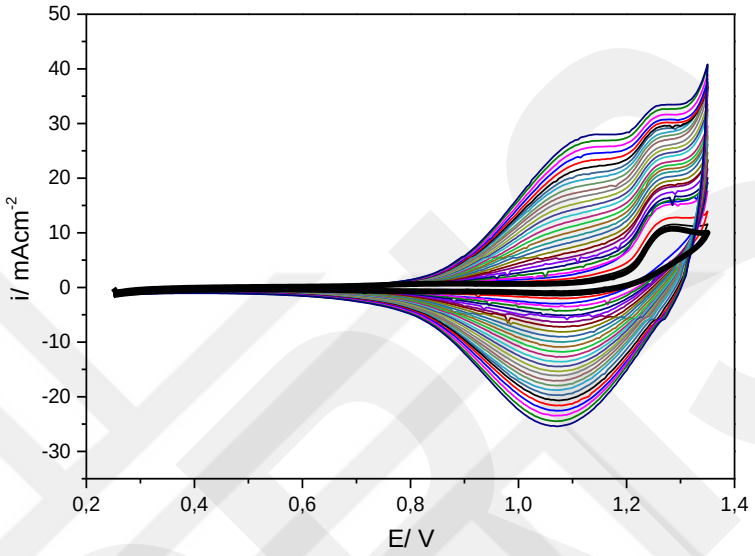

Figure 3.17 Electropolymerization of S_2T-Lum on Pt electrode in 0.1 M TBAH/ACN-BF_3.Et_2O (95:5- v/v) electrolyte solution between 0.25 V and 1.35 V at a scan rate of 100 mV/s

In order to investigate the redox behavior of the polymer film, cyclic voltammograms were taken in a monomer-free electrolyte solution. As shown in Figure 3.18, the PS2T-Lum film represented a reversible redox couple with a half wave of 1.11 V. Also, the current intensity of redox couple increases as a function of scan rates, which confirms non-diffusional redox process and the presence of a well-adhered electroactive polymer film on the electrode surface.

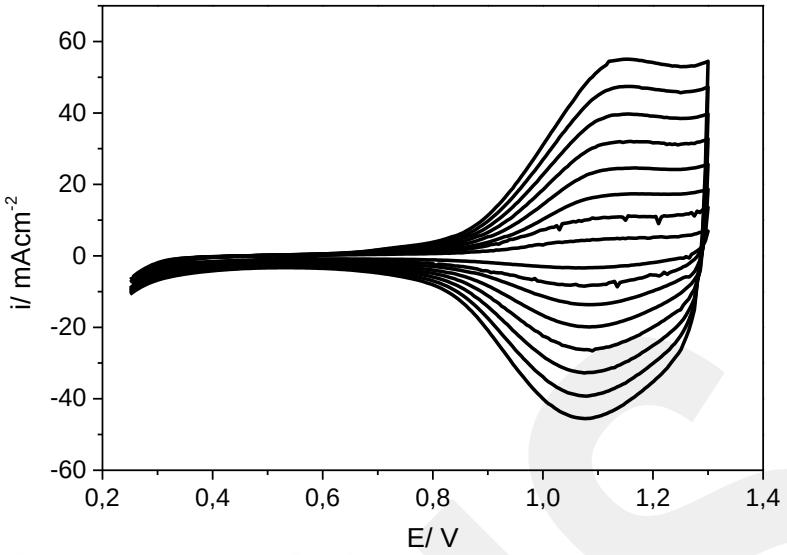

Figure 3.18 Redox behavior of PS_2T-Lum film on Pt electrode in 0.1 M TBAH/ACN-$BF_3.Et_2O$ (95:5- v/v) electrolyte solution between 0.25 V and 1.3 V at various scan rates from 25 mV/s to 200 mV/s with 25 mV/s intervals

3.6 Ion Recognition Properties

In order to get some opinion about the sensitivity of the compounds towards metal ions, the effect of various metal ions on the fluorescence intensity of the compounds was investigated. It was observed that some metals decreased or increased the fluorescence intensity (Figure 3.19, Figure 3.20, Figure 3.21). On the other hand, there was a clear observation of the quenching the fluorescence intensity of the compounds completely in the presence of Cu^{2+} ions. It can be easly concluded that this sensitivity makes them a potential sensor candidate for the recognition of Cu^{2+} ions. Especially, while the fluorescence property of S_2B-Lum is negligible, the radiation is observed in S_2B-Lum material with the addition of metal ions (Figure 3.20).

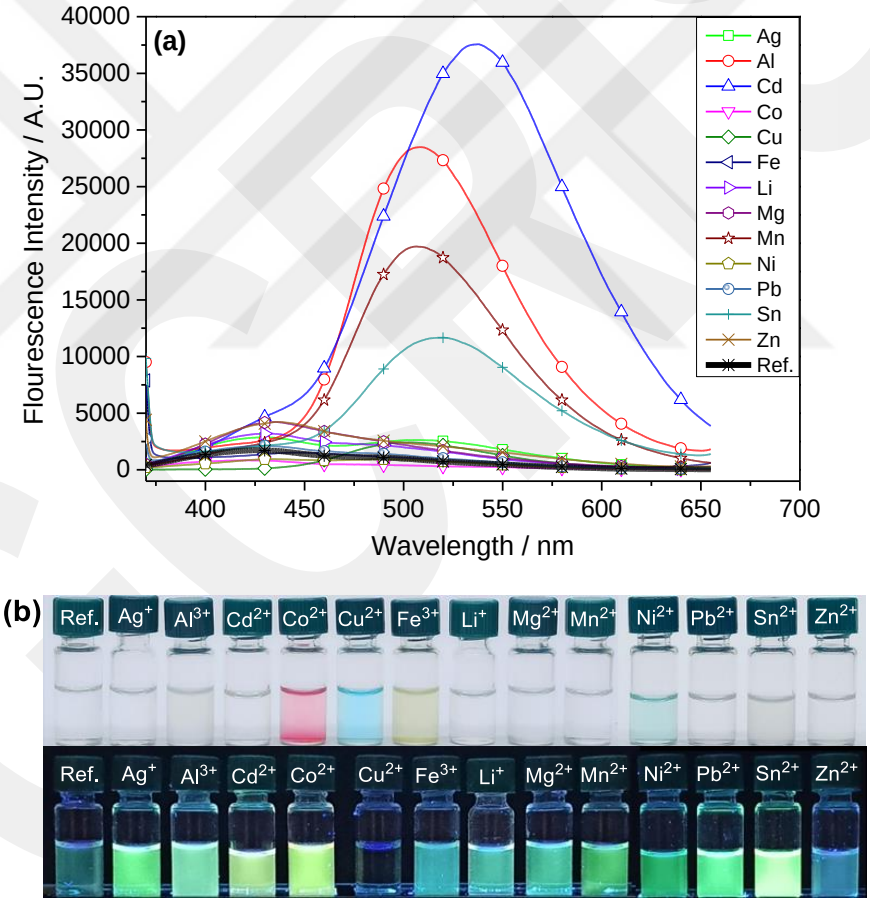

Figure 3.19 (a) Fluorogenic response of F_2B-Lum (10^{-5} M) to various metal ions (0.02 M) and (b) pictures of F_2B-Lum with the metal ions under daylight and UV light (365 nm)

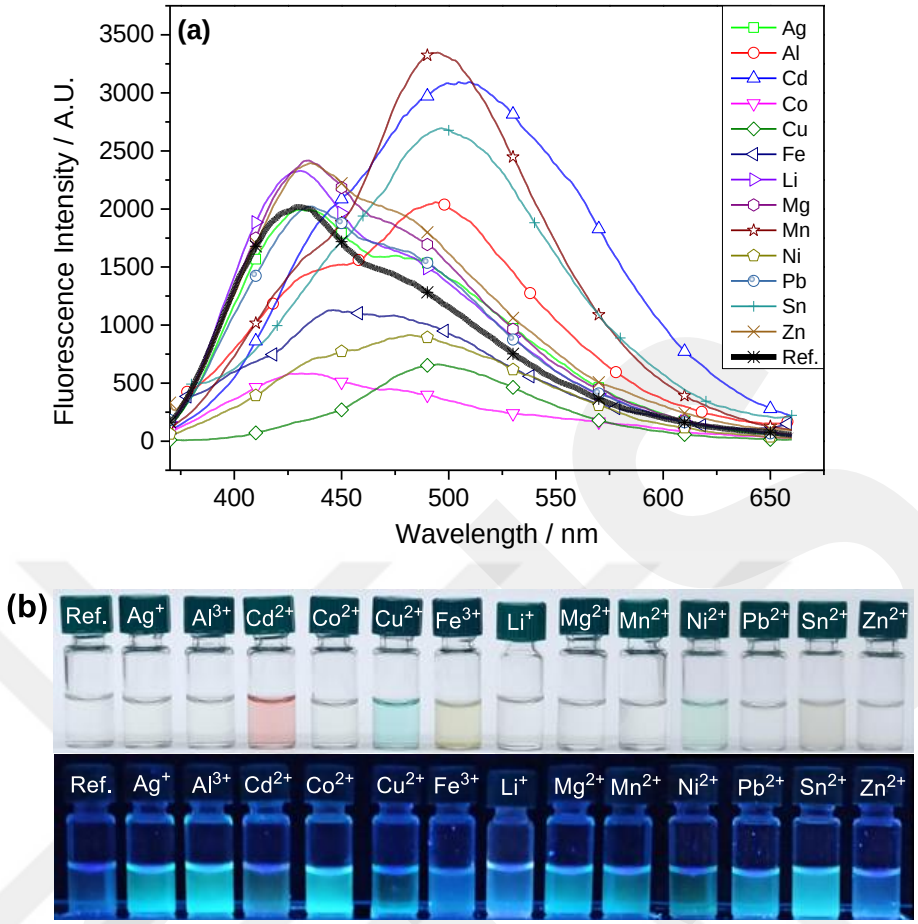

Figure 3.20 (a) Fluorogenic response of S_2B-Lum (10^{-4} M) to various metal ions (0.02 M) and (b) pictures of S_2B-Lum with the metal ions under daylight and UV light (365 nm)

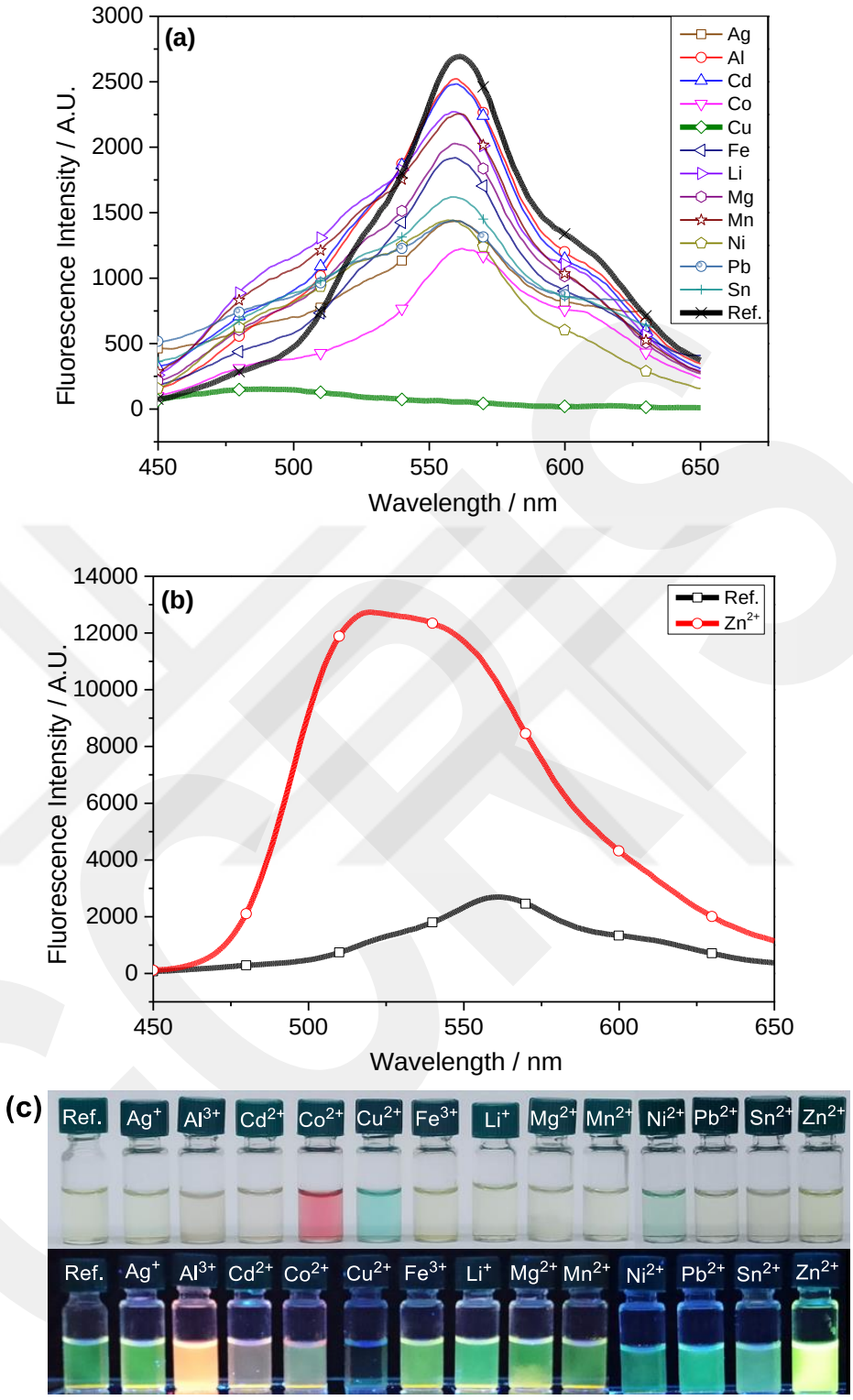

Figure 3.21 (a) Fluorogenic response of S_2T-Lum (10^{-5} M) to various metal ions (0.02 M)(a), (b) fluorogenic response of S_2T-Lum (10^{-5} M) to Zn^{2+} ion and (c) pictures of S_2T-Lum with the metal ions under daylight and UV light (365 nm) (c)

CHAPTER 4

CONCLUSION

In this study, in order to provide new luminol based CL compounds to the literature, a new series of trimeric CL compounds bearing furan and selenophene units have been successfully synthesized in two different ways. The chemical structures of the compounds (F_2B-Lum S_2B-Lum and S_2T-Lum) were characterized by using NMR, HRMS and FTIR techniques. When compared to luminol, the compounds represented low quantum yields, which can be due to the steric effect of furan and selenophene units. This can lead to large dihedral angles between D and A units and also limits the delocalization of electrons in trimeric structure. The CL properties of the compounds were examined by using various oxidants and the best result was obtained using H_2O_2 in basic medium. The CL reaction of the compounds can be catalyzed by using Fe^{3+}, Cu^{2+}, reactive oxygen species, hemin and blood samples. These results make them amenable to use in analytical chemistry and forensic science; for example, they are very sensitive to blood samples even at a 1 to 10.000 dilution of blood. The light formed as a result of the reaction could be seen with the naked eye as a light blue color in a dark environment. On the other hand, by using the fluorescence property of the compound, the presence of the Cu^{2+} ion can be detected by following a decrease in fluorescence intensity. Finally, S_2T-Lum can be polymerized electrochemically and the corresponding electroactive polymer PS_2T-Lum bearing CL appendages can be a precious member of luminol based polymers in the literature.

REFERENCES

[1] M. Browne, "Electromagnetic Waves" *Physics for Engineering and Science*, 2nd ed. Schaum, New York: McGrawHill, 2013, pp. 343-352.

[2] A. Jablonski, "Efficiency of Anti-Stokes Fluorescence in Dyes". *Nature*, vol. 131 pp. 839-840, June 1933.

[3] A.K. Campbell, *Chemiluminescence: Principles and Applications in Biology and Medicine* 1st ed. E. Horwood, Chichester:VCH, 1988, pp. 15-66.

[4] B. P. Chan, "Biomedical Applications of Photochemistry". *Tissue Engineering*, Part B: Reviews, vol. 16, issue 5, pp. 509-522, May 2010.

[5] F. Barni, S. W. Lewis, A. Berti, G.M. Miskelly, G. Lago, "Forensic application of the luminol reaction as a presumptive test for latent blood detection". *Talanta*, vol. 72, issue 3, pp. 896–913, May 2007.

[6] A.M. Garcia-Campana, W.R.G. Baeyens, X. Zhang, "Chemiluminescence-Based Analysis: An Introduction to Principles, Instrumentation, and Applications" in *Chemiluminescence in Analytical Chemistry*. A.M. Garcia-Campana, W.R.G. Baeyens, Eds. United State of America: Marcel Dekker, Inc., 2001, pp. 44-45.

[7] E. N Harvey, "Luminescence of Living Organisms. Bioluminescence" in *A History of Luminescence from the Earliest Times until 1900*. D. Phoenix, Philadelphia: American Philosophical Society, 1957, pp. 457-592.

[8] J. Klein, "The Gooey Details Behind a GlowWorm's Starry Night Illusions". Internet: https://www.nytimes.com/2016/12/16/science/glow-worms-new-zealand.html, 16 December 2016, [26 October 2020].

[9] R. Schreiber, *Firefly Experience*. ArtBook Printing, October 2017.

[10] B. Radziszewski, “Unterrnahnngen uber Eydrobenramid, Amarin and Lophin”. *Chemistry Europe*, vol. 10, issue 1, pp. 70-75, January 1877

[11] G. Lu, J. Wada, T. Kimoto, H. Iga, H. Nishigawa, M. Kimura, & Z. Hu, “The Chemiexcitation of the Chemiluminescence of Lophine Peroxide Anions via a Partially Cyclic Transition State”. *European Journal of Organic Chemistry*, vol 2014, issue 6, pp. 1212-1219, February 2013.

[12] A. J. Schmitz, *Uber des Hydrazyde der Trimensinsaure Pun der Hemimellitsaure*, Heidelberg: Buchdruckerei von J. Hörning, 1913, pp. 39-46.

[13] H.O. Albrecht, “Über die Chemiluminescenz des Aminophthalsäurehydrazids”. *Z. Phys. Chem*. vol. 136 pp. 321-330, July 1928.

[14] M. Rauhut, A. M. Sernsel, B. G. Roberts, “Reaction Rates, Quantum Yields, and Partial Mechanism for the Chemiluminescent Reaction of 3-Aminophthalhydrazide with Aqueous Alkaline Hydrogen Peroxide and Persulfate”. *The Journal of Organic Chemistry*. vol. 31, issue 8, pp.2431-2436, August 1966.

[15] F. Chen, W. Ma, J. He, J. Zhao, “Fenton Degradation of Malachite Green Catalyzed by Aromatic Additives”. *The Journal of Physical Chemistry A*, vol. 106, issue 41, pp. 9485-9490, September 2002.

[16] A. Larena, M. Valero, E. Bernabeu, “Some Chemiluminescence Reactions in Presence of Different Metal Ions”. *Optica Pura y Aplicada*, vol.16, issue 2, pp. 91-96, 1983.

[17] N.W. Barnett, P.S, Francis, “Chemiluminescence: Liquid-Phase”in *Encyclopedia of Analytical Science*, 2nd ed., P. Worsfold, A. Townshend, C. Poole, London: Elsevier Academic Press, 2005, pp. 511-520.

[18] D. M. Hercules, “Chemiluminescence Resulting from Electrochemically Generated Species”. *Science*, vol. 145, pp. 808-809, August 1964.

[19] A.J. Bard, “Introduction” in *Electrogenerated Chemiluminescence*, A.J. Bard, The University of Texas, Austin, Texas, U.S.A., New York: Marcel Dekker, Inc., 2004, pp. 1.

[20] L.R. Faulkner, A.J. Bard, "Techniques of Electrogenerated Chemiluminescence" in *Electroanalytical Chemistry*, A.J. Bard, New York: Marcel Dekker, 1977, vol. 10.

[21] K. A. Fähnrich, M. Pravda, G.G. Guilbault, "Recent Applications of Electrogenerated Chemiluminescence in Chemical Analysis". *Talanta*, vol. 54, pp. 531-599, May 2001.

[22] M.M. Richter, "Electrochemiluminescence (ECL)". *Chem. Rev*. vol. 104, pp. 3003-3036, March 2004.

[23] A. Knight, "A Review of Recent Trends in Analytical Applications of Electrogenerated Chemiluminescence". *TrAC Trends in Analytical Chemistry*, vol. 18, issue 1, pp. 47-62, January 1999.

[24] L.J. Kricka, "Clinical Applications of Chemiluminescence". *Analytica Chimica Acta*, vol. 500(1-2), pp. 279-286, December 2003.

[25] M.J. Navas, A.M. Jime'nez, "Review of Chemiluminescent Methods in Food Analysis". *Food Chem*, vol.55, pp. 7-15, March 1996.

[26] L. G. Gracia, A. M. Garcia-Campana, J. J. S. Chinchilla, J. F. H. Rerez, A. G. Casado, "Analysis of pesticides by chemiluminescence detection in the liquid phase". *TrAC Trends in Analytical Chemistry*, vol. 24, issue 11, pp. 927-942, December 2005.

[27] H. C. McKee, "Collaborative Testing of Methods to Measure Air Pollutants III. The Chemiluminescent Method for Ozone: Determination of Precision". *Journal of the Air Pollution Control Association*, vol. 26, issue 2, pp. 124-128, 1976.

[28] P. Panoutsou, A. Economou, "Rapid enzymatic chemiluminescent assay of glucose by means of a hybrid flow-injection/sequential-injection method". *Talanta*, vol. 67, issue 3, pp. 603-609, September 2005.

[29] M. Hao, N. Liu, Z. Ma, "A new luminol chemiluminescence sensor for glucose based on pH-dependent graphene oxide". *Analyst*, vol. 138, issue 15, pp. 4393-4397, August 2013.

[30] K.D. Gundermann, “Chemiluminescence in Organic Compounds”. *Angewandte Chemie International Edition in English*, vol. 4, issue 7, pp. 566-573, July 1965.

[31] L. A. Burgoyne, “Solid Medium and Method for DNA Storage”. U.S. Patent 5496562, 04 March 1996.

[32] W.R. Seitz, D.M. Hercules, “Determination of trace amounts of iron(II) using chemiluminescence analysis”. *Analytical Chemistry*, vol. 44, issue 13, pp. 2143-2149, November 1972.

[33] H. Ojima, K. Nonoyama, “The mechanism of catalytic chemiluminescence of luminol”. *Studies in Surface Science and Catalysis*, vol. 66, pp. 417-427, 1991.

[34] J.M. Lin, X. Shan, S. Hanaoka, M. Yamada, “Luminol Chemiluminescence in Unbuffered Solutions with a Cobalt(II)−Ethanolamine Complex Immobilized on Resin as Catalyst and Its Application to Analysis”. *Analytical Chemistry,* vol. 73, issue 21, pp. 5043-5051, September 2001.

[35] X. Liu, W. Niu, H. Li, S. Han, L. Hu, G. Xu, “Glucose biosensor based on gold nanoparticle-catalyzed luminol electrochemiluminescence on a three-dimensional sol–gel network”. *Electrochemistry Commun*ications, vol. 10, issue 9, pp. 1250-1253, September 2008.

[36] M. J. Chaichi, M. Ehsani, “A novel glucose sensor based on immobilization of glucose oxidase on the chitosan-coated Fe_3O_4 nanoparticles and the luminol-H_2O_2-gold nanoparticle chemiluminescence detection system”. *Sensors and Actuators B*: *Chemical*, vol. 223, pp. 713-722, February 2016.

[37] Y. Cao, R. Yuan, Y. Chai, H. Liu, Y. Liao, Y. Zhuo, “Amplified cathodic electrochemiluminescence of luminol based on Pd and Pt nanoparticles and glucose oxidase decorated graphene as trace label for ultrasensitive detection of protein”. *Talanta*, vol. 113, pp. 106-112, September 2013.

[38] Y. Cheng, R. Yuan, Y. Chai, H. Niu, Y. Cao, H. Liu, L. Bai, Y. Yuan, “Highly sensitive luminol electrochemiluminescence immunosensor based on ZnO nanoparticles and glucose oxidase decorated graphene for cancer biomarker detection”. *Analytica Chimica Acta*, vol. 745, pp. 137-142, October 2012.

[39] X. Si, X. Song, K. Xu, C. Zhao, J. Wang, Y. Liu, S. He, M. Jin, H. Li, “Bovine serum albumin-templated MnO_2 nanoparticles are peroxidase mimics for glucose determination by luminol chemiluminescence”. *Microchemical Journal*, vol. 149, pp. 104050-104051, September 2019.

[40] Y-H. Wang, F-L. Li, Y-Q. Wang, S. Wu, X-X. He, K-M. Wang, “A TiO_2/CNTs Nanocomposites Enhanced Luminol Electrochemiluminescence Assay for Glucose Detection”. *Chinese Journal of Analytical Chemistry*, vol. 43, issue 11, pp. 1682–1687, November 2015.

[41] W. Specht, “Die Chemiluminescenz des Hämins, ein Hilfsmittel zur Auffindung und Erkennung forensisch wichtiger Blutspuren”. *Angew. Chem.*, vol. 50, pp. 155-157, 1937.

[42] H. M. Nunno, “Forensic DNA Analysis” in *Forensic Chemistry Handbook*. L. Kobilinsky, Ed. United States of America: A John Wiley & Sons, Inc., Publication, 2011, pp. 291-326.

[43] Compound Interest, “Crime Scene Chemistry-Luminol, Blood & Horseradish”, Internet: https://www.compoundchem.com/2014/10/17/luminol/, 2014.

[44] F. Garnier, G. Tourillon, M. Gazard, J. C. Dubois, "Organic conducting polymers derived from substituted tiophenes as electrochromic material". *Journal of Electroanalytical Chemistry*, vol. 148, issue 2, pp. 299-303, June 1983.

[45] J. W. Thackeray, H. S. White, M. S. Wrighton, “Poly(3-methylthiophene)-coated electrodes: optical and electrical properties as a function of redox potential and amplification of electrical and chemical signals using poly(3-methylthiophene)-based microelectrochemical transistors”. *Journal of Physical Chemistry*, vol. 89, issue 23, pp. 5133-5140, November 1985.

[46] H. Koezuka, A. Tsumura, T. Ando, “Field-effect transistor with polythiophene thin film”. *Synthetic Metals*, vol. 18, issues 1-3, pp. 699-704, February 1987.

[47] S. Glenis, G. Horowitz, G. Tourillon, F. Garnier, “Electrochemically grown polythiophene and poly(3-methylthiophene) organic photovoltaic cells”. T*hin Solid Films*, vol. 111, issue 2, pp. 93-103, January 1984.

[48] P.J. Kinlen, B.G. Frushour, Y. Ding, V. Menor, “Synthesis and Characterization of Organically Soluble Polyaniline and Polyaniline Block Copolymers”. *Synthetic Metals*, vol. 101, issues 1-3, pp. 758-761, May 1999.

[49] J. Lee, H. H. Seliger, “Absolute Spectral Sensitivity of Phototubes and The Application to The Measurement of The Absolute Quantum Yields of Chemiluminescence And Bioluminescence”. *Photochemistry and Photobiology*, vol. 4, issue 6, pp. 1015-1048, December 1965.

[50] D. F. Roswell, E. H. White, “The chemiluminescence of luminol and related hydrazides”. *Methods in Enzymology*, vol. 57, pp. 409–423, 1978.

[51] H. D. K. Drew and F. H. Pearman, “Chemiluminescent organic compounds. Part IV. Amino- and hydrazino-cyclophthalhydrazides and their relative luminescent power”. *Journal of the Chemical Society*, pp. 586-592, 1937.

[52] K.-D. Gundermann, “Recent advances in research on the chemiluminescence of organic compounds”. *Top. Curr. Chem*. vol. 46, pp. 61-139, 1974.

[53] C. C. Wei, E. H. White, “An efficient chemiluminescent hydrazide: benzo(ghi)perylene-1,2-dicarboxylic acid hydrazide”. *Tetrahedron Letters*, vol. 12, issue 39, pp. 3559-3562, August 1971.

[54] D. F. Roswell, V. Paul, E. H. White, “Energy transfer in chemiluminescence. II”. *Journal of the American Chemical Society*, vol. 92, issue 16 pp. 4855-4860, August 1970.

[55] D. Asil, A. Cihaner, F. Algı, A. M. Önal, “A Diverse-Stimuli Responsive Chemiluminescent Probe with Luminol Scaffold and Its Electropolymerization”. *Electroanalysis*, vol. 22, issue 19, pp. 2254-2260, July 2010.

[56] D. Asil, A. Cihaner, A. M. Önal, “Electropolymerization and ion sensitivity of chemiluminescent thienyl systems”. *Electrochimica Acta*, vol. 54, issue 26, pp. 6740-6746, November 2009.

[57] A. Degirmenci, F. Algi, "Synthesis, chemiluminescence and energy transfer efficiency of 2,3-dihydrophthalazine-1,4-dione and BODIPY dyad". *Dyes and Pigments* vol. 140, pp. 92-99, May 2017.

[58] S. Deepa, S. Rajasekhara Reddy, K. Rajendrakumar, "Green Chemiluminescence of Highly Fluorescent Symmetrical Azo-Based Luminol Derivative". *Oriental Journal of Chemistry*, vol 34, issue 2, pp. 894-905, April 2018.

[59] G. Periyasami, L, Martelo, C. Baleizão, M. N. Berberan-Santos, "Strong green chemiluminescence from naphthalene analogues of luminol". *New Journal of Chemistry*, vol. 38, issue 6, pp. 2258-2261, March 2014.

[60] T. F. Jiao, Y. Y. Xing, J. X. Zhou, W. Wang, "Synthesis and Characterization of Some Functional Luminol Derivatives with Aromatic Substituted Groups". *Advanced Materials Research*, vol. 197-198, pp. 606-609, February 2011.

[61] J. Han, J. Jose, E. Mei, K. Burgess, "Chemiluminescent Energy-Transfer Cassettes Based on Fluorescein and Nile Red". *Angewandte Chemie International Edition*, vol. 46, pp. 1684–1687, February 2007.

[62] A. Spruit-van der Burg, "Emission spectra of some chemoluminescent reactions. Part II. The oxidation of derivatives of 2,3-dihydrophthalazine-1,4-dione". *Recueil des Travaux Chimiques des Pays-Bas*, vol. 69, issue 12, pp. 1536-1544, 1950.

[63] D. Asil, A. Cihaner, A. M. Önal, "A glow in the dark: synthesis and electropolymerization of a novel chemiluminescent terthienyl system". *Chemical Communications*, pp. 307-309, December 2009.

[64] N. Atılgan, F. Algı, A. M. Onal, A. Cihaner, "Synthesis and properties of a novel redox driven chemiluminescent material built on a terthienyl system". *Tetrahedron*, vol. 65, pp. 5776-5781, July 2009.

[65] P. Beauchamp, "Infrared Tables". Spectroscopy Tables, Department of Chemistry, Cal Poly Pomona, California.

[66] J. R. Lakowicz, "Instrumentation for Fluorescence Spectroscopy" in *Principles of Fluorescence Spectroscopy*, 2nd ed. New York: Kluwer Academic/Plenum, 1999, pp. 52-53.

[67] H. Yang, M. Li, C. Li, Q. Luo, M. Q. Zhu, H. Tian, W. H. Zhu, “Unraveling Dual Aggregation-Induced Emission Behavior in Steric-Hindrance Photochromic System for Super Resolution Imaging”. *Angewandte Chemie International Edition*, vol. 59, issue 22, pp. 8560-8570, September 2019.

[68] A. Bukauskytė, R. Karpicz, R. Striela, L. Labanauskas, A. Gruodis, D. Peckus, R. Augulis, V. Gulbinas, “The Influence of Substituents of Perylenediimides on Their Spectroscopic Properties”. *Journal of Luminescence*, vol. 195, pp. 252–258, March 2018.

[69] A. M. Brouwer, "Standards for photoluminescence quantum yield measurements in solution (IUPAC Technical Report)". *Pure and Applied Chemistry*, vol. 83 issue 12, pp. 2213–2228, January 2011.

[70] B. Halliwella, M. V. Clement, L. H. Long, “Hydrogen peroxide in the human body”. *FEBS Letters*, vol. 486, issue 1, pp. 10-13, December 2000.

[71] A. Sachs, V. E. Levine, F. C. Hill, and R. Hughes, “Copper and Iron in Human Blood”. *Archives of Internal Medicine*, vol. 71, issue 4, April 1943.

[72] M. Bibi, M.Z. Hashmi, R.N. Malik, “The level and distribution of heavy metals and changes in oxidative stress indices in humans from Lahore district, Pakistan”. *Human and Experimental Toxicology*, vol. 35, issue 1, pp. 78-90, March 2015.

APPENDICES

A. NMR RESULTS

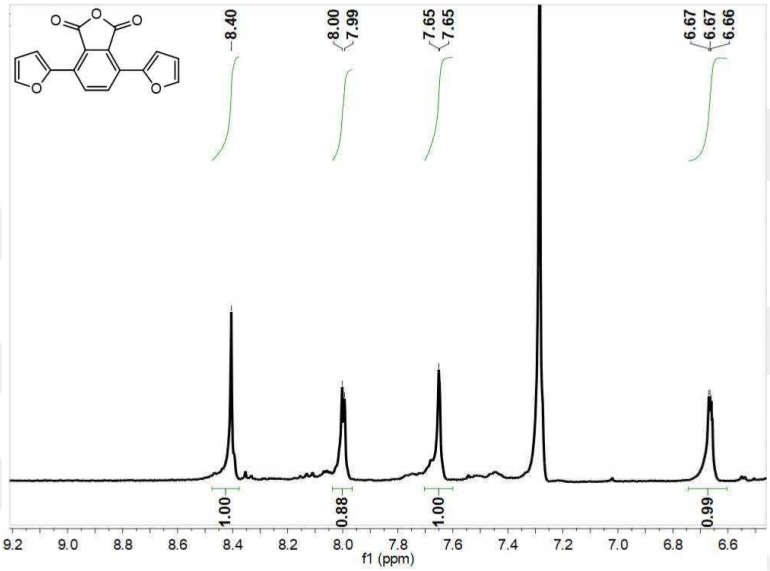

Figure A.1 ^{1}H NMR spectrum of F_2-PA in $CDCl_3$

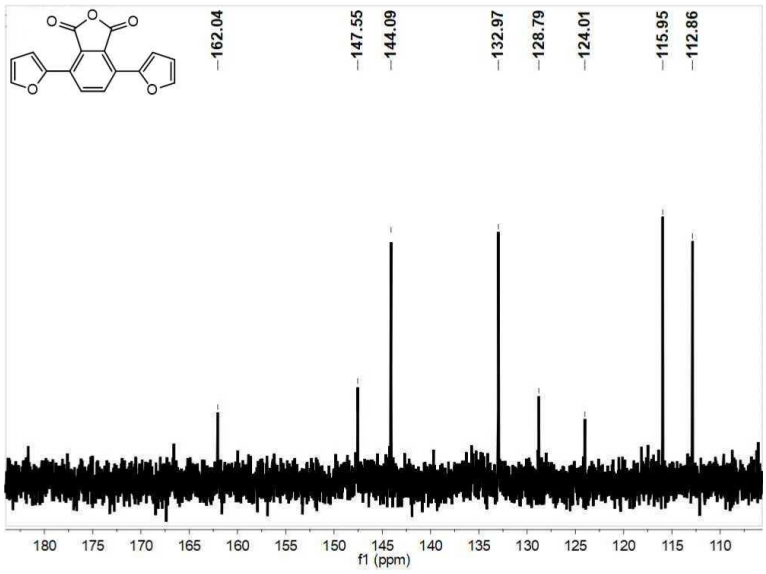

Figure A.2 .^{13}C NMR spectrum of F_2-PA in $CDCl_3$

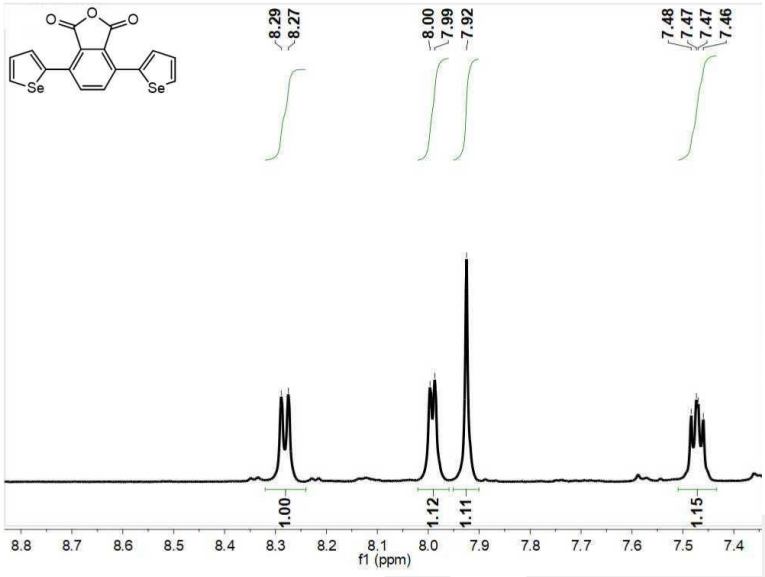

Figure A.3 ^{1}H NMR spectrum of S_2-PA in $CDCl_3$

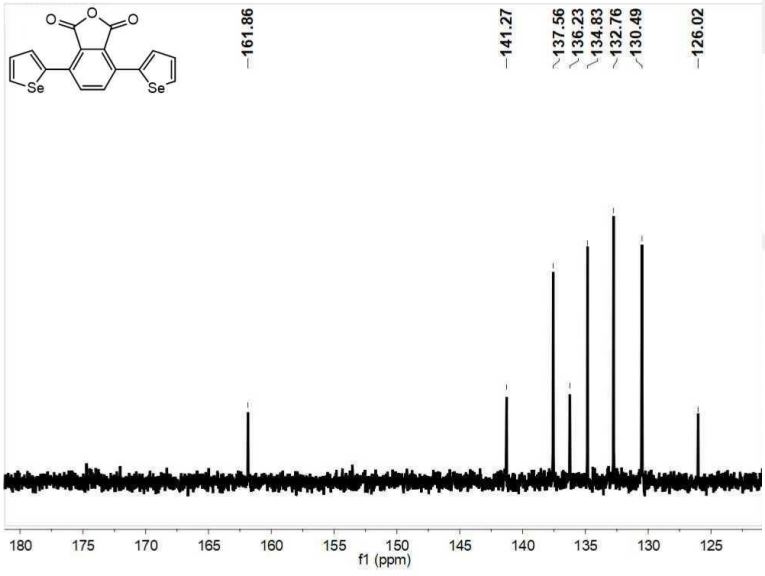

Figure A.4 ^{13}C NMR spectrum of S_2-PA in $CDCl_3$

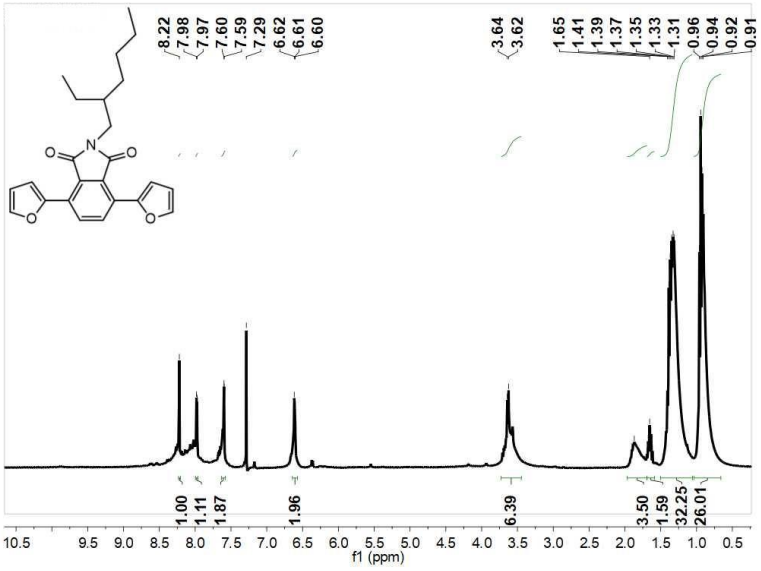

Figure A.5 ^{1}H NMR spectrum of F_2-PI-EtHex in $CDCl_3$

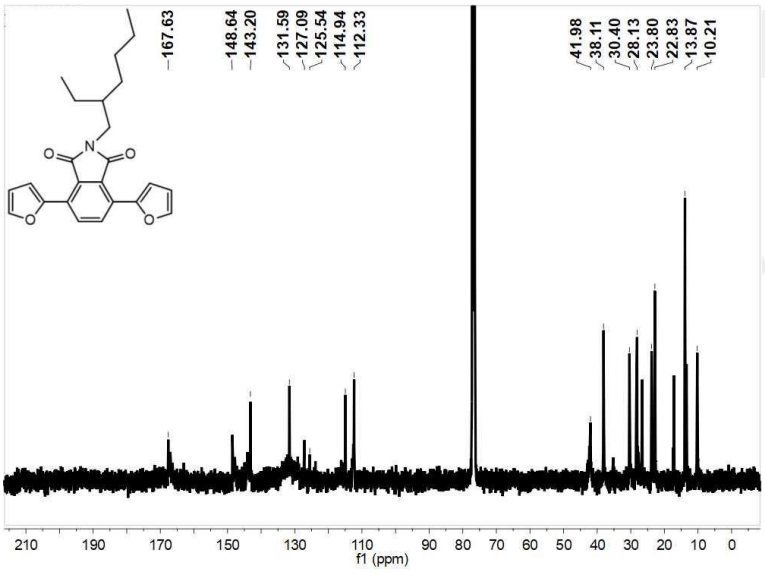

Figure A.6 ^{13}C NMR spectrum of F_2-PI-EtHex in $CDCl_3$

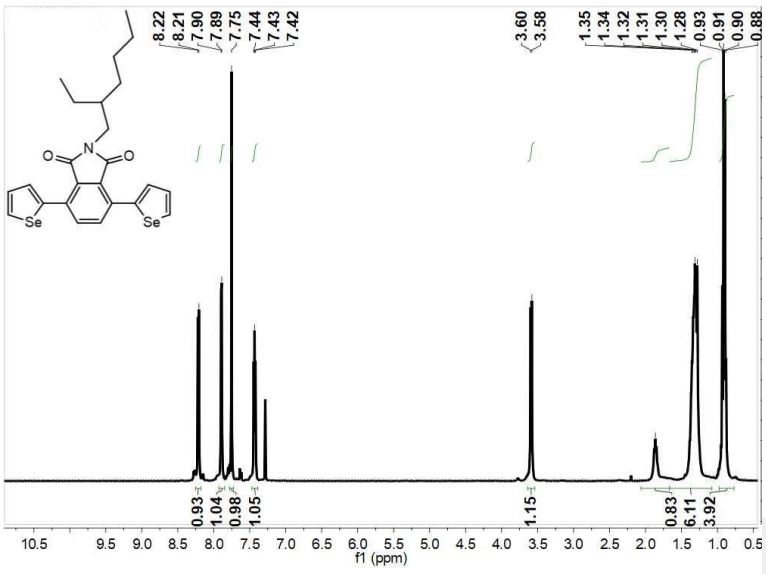

Figure A.7 ^{1}H NMR spectrum of S_2-PI-EtHex in $CDCl_3$

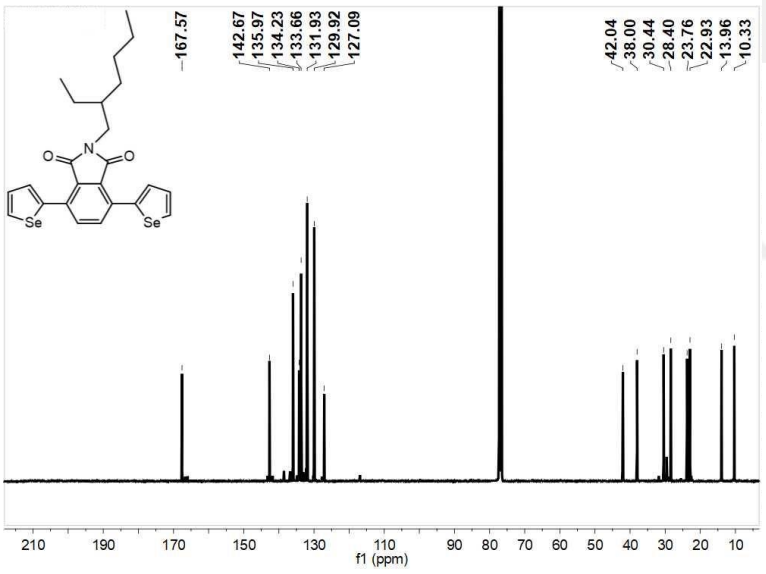

Figure A.8 ^{13}C NMR spectrum of S_2-PI-EtHex in $CDCl_3$

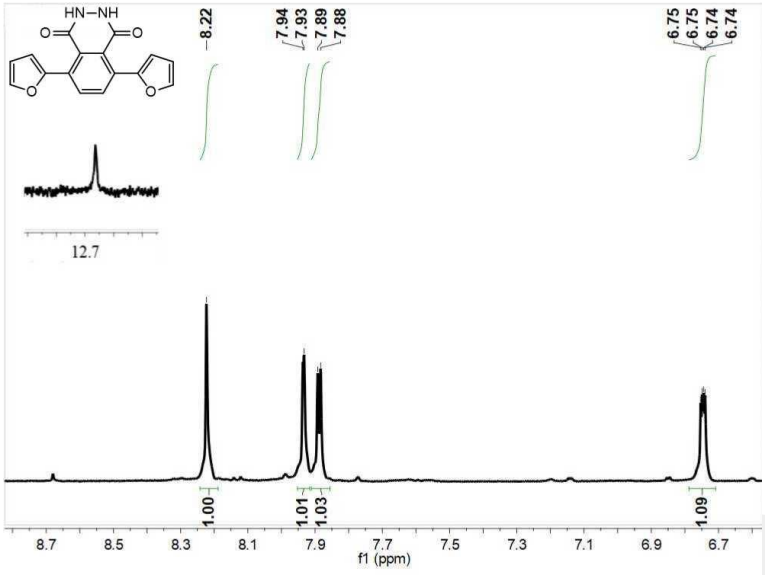

Figure A.9 ^{1}H NMR spectrum of F_2B-Lum in DMSO

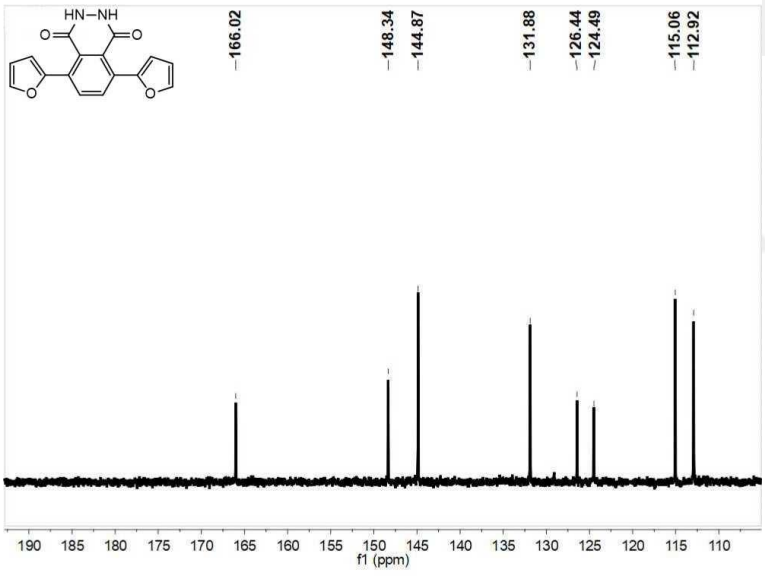

Figure A.10 ^{13}C NMR spectrum of F_2B-Lum in DMSO

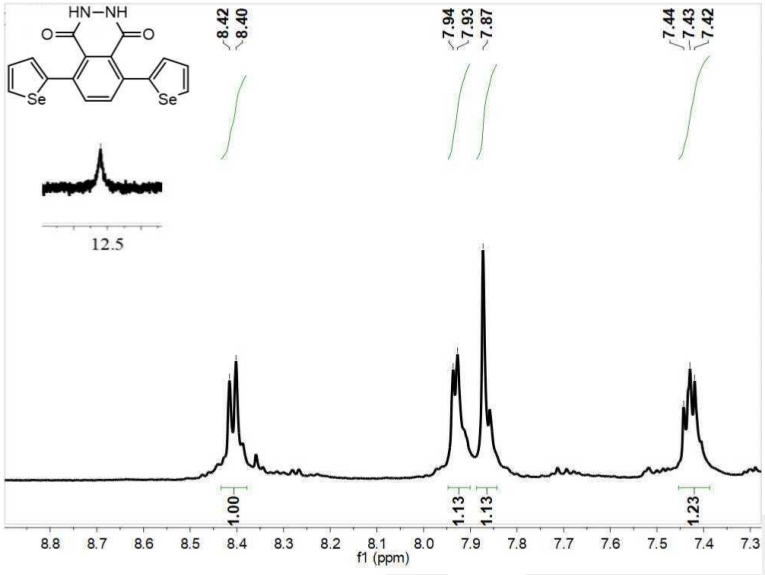

Figure A.11 ^{1}H NMR spectrum of S_2B-Lum in DMSO

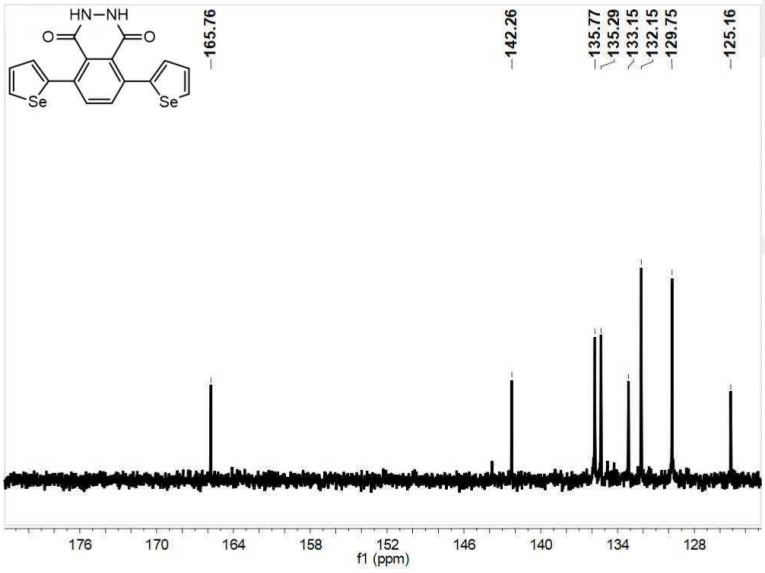

Figure A.12 ^{13}C NMR spectrum of S_2B-Lum in DMSO

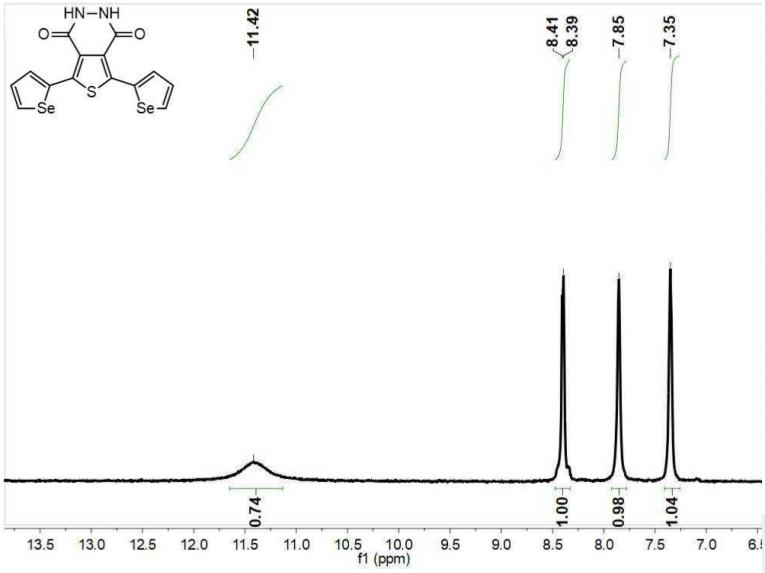

Figure A.13 ^{1}H NMR spectrum of S_2T-Lum in DMSO

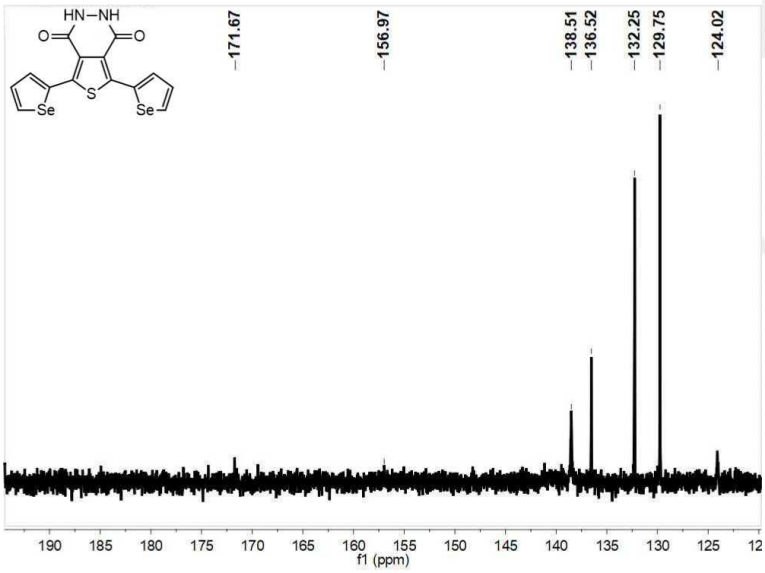

Figure A.14 ^{13}C NMR spectrum of S_2T-Lum in DMSO.

B. FTIR RESULTS

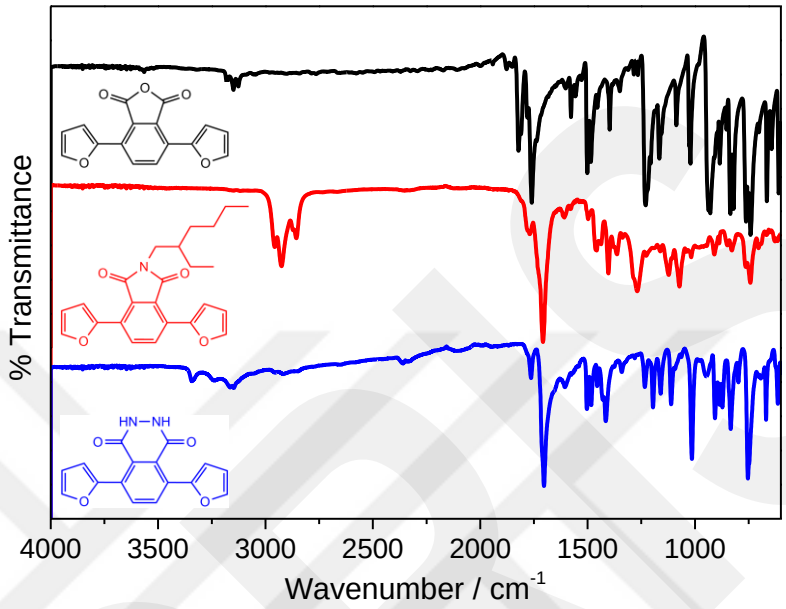

Figure B.1 FTIR spectra of F_2-PA, F_2-PI-EtHex and F_2B-Lum

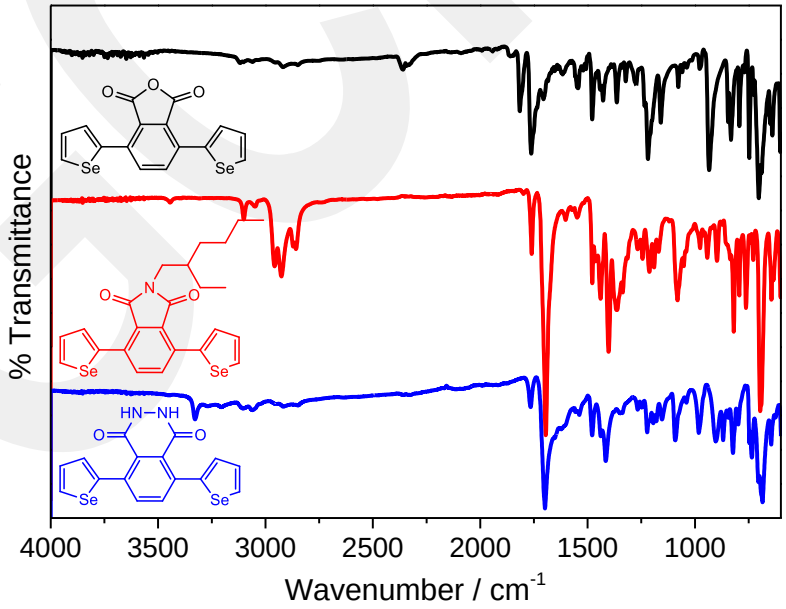

Figure B.2 FTIR spectra of S_2-PA, S_2-PI-EtHex and S_2B-Lum

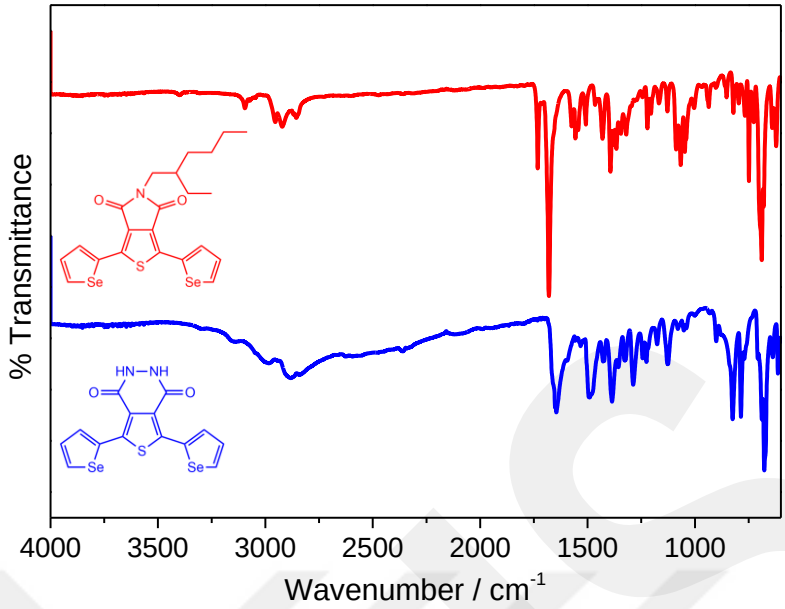

Figure B.3 FTIR spectra of S_2-TPD-EtHex and S_2T-Lum

C. HRMS RESULTS

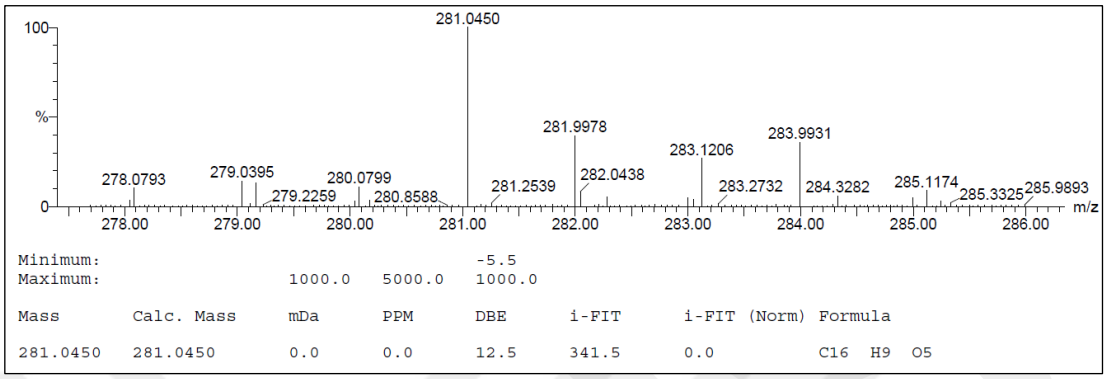

Minimum:				-5.5			
Maximum:		1000.0	5000.0	1000.0			
Mass	Calc. Mass	mDa	PPM	DBE	i-FIT	i-FIT (Norm)	Formula
281.0450	281.0450	0.0	0.0	12.5	341.5	0.0	C16 H9 O5

Figure C.1 HRMS spectrum of F_2-PA

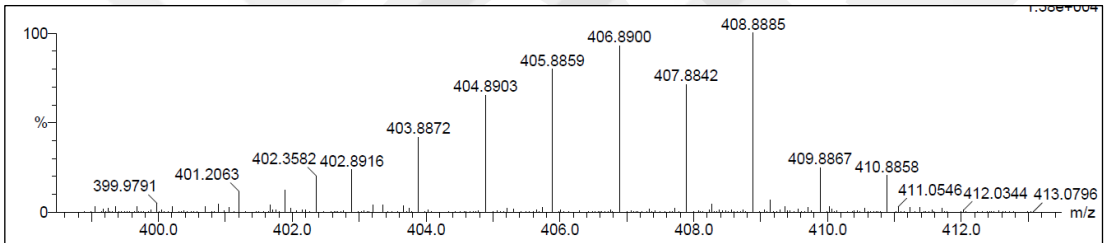

Minimum:				-5.5					
Maximum:		1000.0	5000.0	1000.0					
Mass	Calc. Mass	mDa	PPM	DBE	i-FIT	i-FIT (Norm)	Formula		
406.8900	406.8890	1.0	2.5	14.5	384.2	0.7	C16 H9 O3	78Se	80Se
	406.8911	-1.1	-2.7	14.5	384.2	0.7	C16 H9 O3	76Se	82Se

Figure C.2 HRMS spectrum of S_2-PA

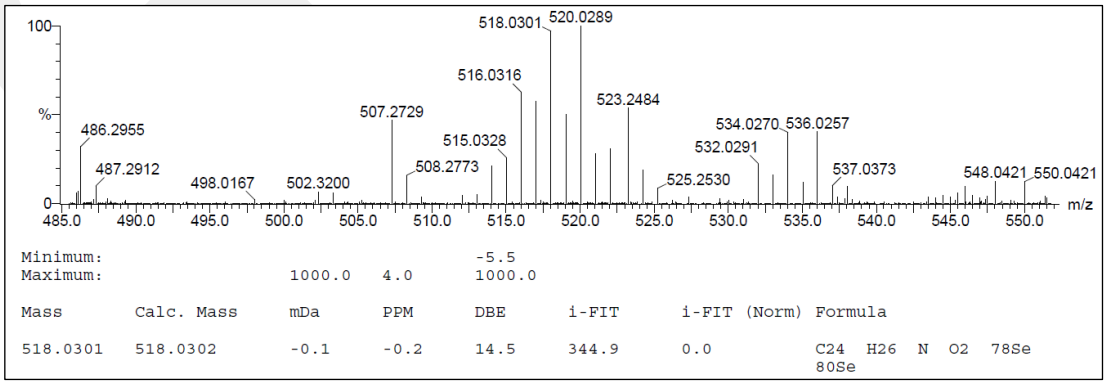

Minimum:				-5.5			
Maximum:		1000.0	4.0	1000.0			
Mass	Calc. Mass	mDa	PPM	DBE	i-FIT	i-FIT (Norm)	Formula
518.0301	518.0302	-0.1	-0.2	14.5	344.9	0.0	C24 H26 N O2 78Se 80Se

Figure C.3 HRMS spectrum of S_2-PI-EtHe

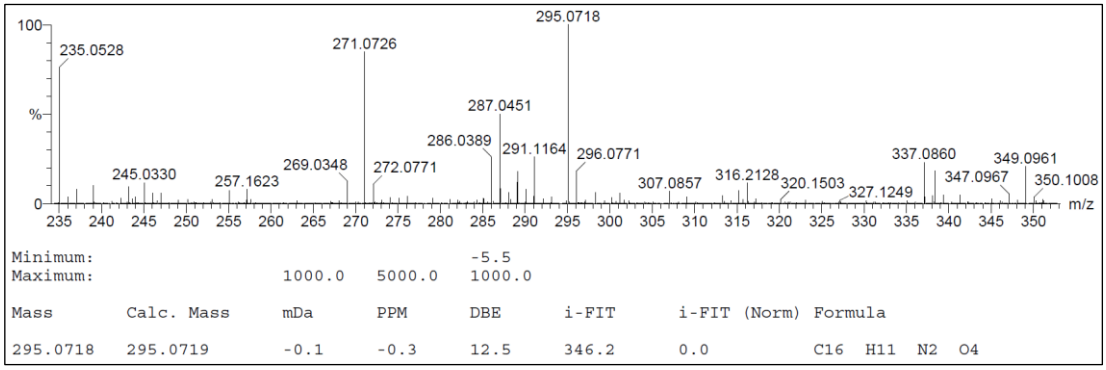

Minimum:				-5.5			
Maximum:		1000.0	5000.0	1000.0			
Mass	Calc. Mass	mDa	PPM	DBE	i-FIT	i-FIT (Norm)	Formula
295.0718	295.0719	-0.1	-0.3	12.5	346.2	0.0	C16 H11 N2 O4

Figure C.4 HRMS spectrum of F_2B-Lum

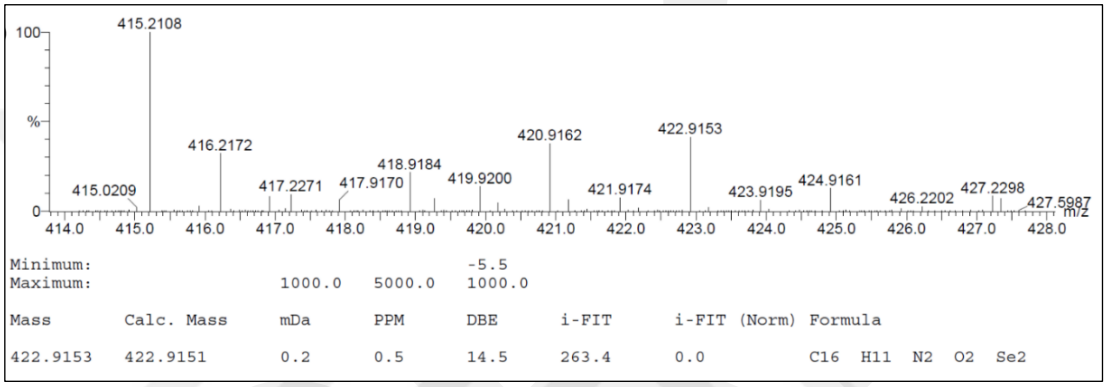

Minimum:				-5.5			
Maximum:		1000.0	5000.0	1000.0			
Mass	Calc. Mass	mDa	PPM	DBE	i-FIT	i-FIT (Norm)	Formula
422.9153	422.9151	0.2	0.5	14.5	263.4	0.0	C16 H11 N2 O2 Se2

Figure C.5 HRMS spectrum of S_2B-Lum

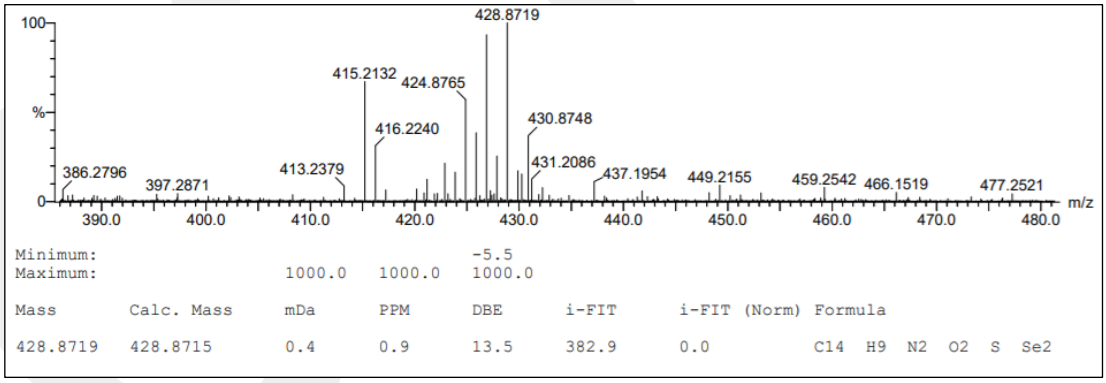

Minimum:				-5.5			
Maximum:		1000.0	1000.0	1000.0			
Mass	Calc. Mass	mDa	PPM	DBE	i-FIT	i-FIT (Norm)	Formula
428.8719	428.8715	0.4	0.9	13.5	382.9	0.0	C14 H9 N2 O2 S Se2

Figure C.6 HRMS spectrum of S_2T-Lum